JAERI-Research
97-031

# STUDY OF IDENTIFICATION OF GEOMETRICALLY SHAPED SOLIDS USING COLOUR AND RANGE INFORMATION

May 1997

Kenichi EBIHARA

日本原子力研究所
Japan Atomic Energy Research Institute

本レポートは，日本原子力研究所が不定期に公刊している研究報告書です。
入手の問合わせは，日本原子力研究所研究情報部研究情報課（〒319-11 茨城県那珂郡東海村）あて，お申し越しください。なお，このほかに財団法人原子力弘済会資料センター（〒319-11 茨城県那珂郡東海村日本原子力研究所内）で複写による実費頒布をおこなっております。

This report is issued irregularly.
Inquiries about availability of the reports should be addressed to Research Information Division, Department of Intellectual Resources, Japan Atomic Energy Research Institute, Tokai-mura, Naka-gun, Ibaraki-ken 319-11, Japan.



編集兼発行　日本原子力研究所
印　　刷　㈱原子力資料サービス

JAERI－Research 97－031

# Study of Identification of Geometrically Shaped Solids Using Colour and Range Information

Kenichi EBIHARA

Center for Promotion of Computational Science and Engineering
Japan Atomic Energy Research Institute
Tokai-mura, Naka-gun, Ibaraki-ken

(Received April 1, 1997)

This report is the revision of the Technical Report (MECSE 1996-7) of Monash University in Melbourne, Australia which has been distributed to the Department Library in this University. The main work which is described in this report was carried out at Intelligent Robotics Research Center (IRRC) in the Department of Electrical and Computer Systems Engineering of Monash University from March in 1995 to March in 1996 and was be supported by a grant from Research Development Corporation of Japan (JRDC).

This report describes the study of identification of geometrically shaped solids with unique colour using colour and range information. This study aims at recognition of equipment in nuclear plants. For this purpose, it is hypothesized that equipment in nuclear plants can be represented by combination of geometrically shaped solids with unique colour, such as a sphere, an ellipsoid, a cone, a cylinder, a rectangular solid and a pyramid. In this report, the colour image of geometrically shaped solids could be segmented comparatively easily and effectively into regions of each solid by using colour and range information. The range data of each solid was extracted using the segmented colour image. Thus the extracted range data could be classified into a plane surface or a curved surface by checking its spatial distribution.

Keywords: Image Segmentation, Sensor Fusion, Geometrically Shaped Solids, Equipment Recognition, Image Processing, Rangefinder

# カラー情報と距離情報を用いた幾何学的形状立体の同定に関する研究

日本原子力研究所計算科学技術推進センター
海老原健一

（1997年4月1日受理）

本報告書は，オーストラリア，メルボルンのモナッシュ大学へ提出したテクニカルレポートをJAERI-Research用に書き換えたものである。なお提出されたテクニカルレポートは，MECSE 1996-7として，同大学の工学部電気計算機システム学科の図書館に配付されている。

本報告書において記述されている主な仕事は，同大学同学科の知能ロボット研究センター（IRRC）において，筆者が，1995年の4月から1996年の3月までに，新技術事業団の海外派遣研究員として行なったものである。

本報告書では，カラー画像の色情報及び距離情報を用いて，単一色の幾何学的形状の物体の同定の研究について記述している。本研究は，原子力施設内の機器の認識を目指しており，そのため，施設内の機器は，単一色の幾何学的形状の組み合わせで表現できると仮定している。幾何学的形状の立体としては，球，楕円体，円錐，円柱，直方体，角錐を使用した。今回の研究では，色情報と距離情報を用いて，幾何学的形状立体のカラー画像が，比較的容易かつ効果的に，各立体の領域に分割することが可能となった。さらに，この領域分割されたカラー画像を用いて，各立体の距離データを抽出し，それら抽出された距離データは，その空間分布を調べることにより，平面と曲面に分類される。

日本原子力研究所：〒319-11　茨城県那珂郡東海村白方白根2－4

Contents

1. Introduction ..... 1
2. Colour Image and Range Data ..... 2
2.1 Laser Scanning Rangefinder and Range Data ..... 2
2.2 Colour CCD Camera and Colour Image ..... 3
3. Noise Reduction from Range Data ..... 5
3.1 Definition of Noise Included in Range Data ..... 5
3.2 Supplement of Lack of Range Data ..... 6
3.3 Reduction of Noise Due to Measurement Error ..... 6
4. Colour Image Segmentation Using Range and Colour Information ..... 13
4.1 Outline of Fusion of Colour and Range Information ..... 13
4.2 Background Elimination from Colour Image ..... 13
4.3 Colour Image Segmentation Using Hue and Saturation ..... 13
4.4 Colour Image Resegmentation Using the Normal Vector ..... 15
5. Identification of Geometrically Shaped Solids ..... 25
6. Conclusions and Discussions ..... 39
7. Future works ..... 40
Acknowledgements ..... 41
Reference ..... 41
Appendix ..... 42

# 目　　次

1. はじめに …… 1
2. カラー画像と距離データ …… 2
2.1 レーザー走査レンジファインダーと距離データ …… 2
2.2 カラーＣＣＤカメラとカラー画像 …… 3
3. 距離データからのノイズ除去 …… 5
3.1 距離データに含まれるノイズの定義 …… 5
3.2 欠如した距離データの補間 …… 6
3.3 測定誤差によるノイズの平滑化 …… 6
4. 距離情報及び色情報を用いたカラー画像分割 …… 13
4.1 色情報と距離情報の融合の概要 …… 13
4.2 カラー画像からの背景除去 …… 13
4.3 色相及び彩度を用いた色画像分割 …… 13
4.4 法線ベクトルを用いたカラー画像の再分割 …… 15
5. 幾何学的形状立体の同定 …… 25
6. 結果と考察 …… 39
7. 今後の研究 …… 40
謝　　辞 …… 41
参考文献 …… 41
付　　録 …… 42

# 1. Introduction

This report describes the study of identification of geometrically shaped solids in environment using colour and range information. The geometrically shaped solids are a sphere, an ellipsoid, a cone, a cylinder, a pyramid and a rectangular solid which have their own unique colour respectively. The purpose of this study is recognition of equipment in nuclear plants under the assumption that equipment in nuclear plants consists of geometrically shaped solids. Therefore the developed program in this study can be considered as one first step for realization of equipment recognition in nuclear plants.

In the developed program, the colour image could be segmented into several regions of each geometrically shaped solid comparatively easily and effectively by using colour information, which is included in a colour image, and range information, which is distance to objects from the measurement instrument. Using the segmented colour image, range data of each solid could be extracted from a whole range data and the analytical surface equation was fitted to the extracted range data for identifying each solids. Especially range information played the useful role for segmentation of the colour image. This is one type of the concept of sensor fusion[1], that is to say fusion of colour information and range information. Colour information and range information are also used effectively in the recognition process of human's. Then it may be natural idea to use both colour information and range information for colour image segmentation and identification of each solid.

The next section describes instruments for taking the colour image and range data as well as showing the taken colour image and range data. In the third section, noise reduction from range data is described. The process and several results of segmentation of the colour image is written in the fourth section. Possibility for identification of each geometrically shaped solids is described in fifth section. In the last two sections, this report is concluded and future works are discussed.

# 2. Colour Image and Range data

In this section, the colour CCD camera and the laser-scanning rangefinder which were used in this project are described. The colour image and range data are also shown.

## 2.1 Laser Scanning Rangefinder and Range Data

In this project, the laser Scanning Rangefinder[2] which was developed by K.Ajay for mobile robot navigation is used as an instrument for measuring distance. This rangefinder comprises the laser projector which projects infrared light to the surface of objects and the monochrome CCD camera which detects reflected light from the surface because of using triangulation principle for measuring distance. The monochrome CCD camera and the laser projector is set on a tripod. The baseline length between the monochrome CCD camera and the laser projector is 46.5 cm. The picture of this rangefinder is shown in Figure 2.1 (a).

The monochrome CCD camera is a commercial one and the laser projector was developed in Monash University. The monochrome CCD camera is JE7352 which was produced by JAVELIN ELECTRONICS. This camera has 1/2 inches CCD element inside and is equipped with the lens produced by COSMICAR whose focus length and F value are 6mm and F1:1.2 respectively. One filter for detecting reflected infrared light which is invisible is attached to this lens. The laser projector generates infrared light which is 20mW at 830mm. This infrared light is collimated in the shape of a vertical stripe using the half-cylindrical lens which can rotate around a vertical axis for scanning the vertical light stripe horizontally.

The monochrome CCD camera and the laser projector are connected to a special processing board which was designed and developed in Monash University. The main functions of this board are to control the half-cylindrical lens in the projector and to detect the image of reflected strip light. This board which is attached to a ISA bus of IBM PC clone computer is one characteristic of this laser scanning rangefinder for measuring distance so quickly because the light stripe detection in taken images is carried out on this board, that is hardware, instead of software.

Lookup tables for outputting range images is another characteristic of this rangefinder system. In triangulation principle, the direction angles of projected light, the position of reflected light in the taken image and the baseline length are necessary factors for calculation of distance. Although range is usually calculated every measurement using these factors, lookup tables are referred for obtaining range data in this rangefinder system. Therefore it is fast to have range data at each pixel in the range image. These lookup tables are generated using the image of the special calibration frame which is shown in Figure 2.2. Two kinds of special software have been developed for generating these lookup tables. One is GUI software which runs on DOS and is used to have data for determining the relative position between the rangefinder and 3-dimensional coordinate system which is attached on the calibration frame. The other is for generating lookup tables using data obtained by above software.

This rangefinder system can output a range image which is called a 2 1/2 dimensional image and range data in the 3-dimensional coordinate system using the special GUI software. The

range image is convenient to apply window operators which is used in general image processing for intensity images. The resolution of the range image is 256 × 256 and the range level is 256. One unit of this range level corresponds 1cm in real distance and measurable distance in this system is from 50cm to 306cm. The range data in the 3-dimensional coordinate system can be used for identifying the real position and the surface shape of objects. Hence, in this project, the range image was used for fusion with a corresponding colour image and noise reduction and the 3-dimensional range data is used for identifying the surface shape of objects. The sample range image and the corresponding range data in the 3-dimensional coordinate system are shown in Figure 2.3 (a), (b).

## 2.2 Colour CCD Camera and Colour Image

The colour CCD camera(Figure 2.1 (b)) is VIC-2974 which is produced by SANYO Electric Co. Ltd. and has one 2/3 inches CCD element inside. The lens produced by KOWA whose focus length and F value are 6mm and F1:1.4 respectively is equipped to this colour CCD camera. This colour CCD camera is also set on a different tripod from that of the rangefinder system and is connected to the colour image grabber board which is MATROX COMET produced by MATROX Electronic System, Ltd.

The software for detecting colour image is written using MATROX's special library which is the set of C like functions and runs on DOS. The resolution of the colour image detected by this colour CCD camera is 256 × 256 and the colour intensity level of red, green and blue is 256 respectively. The sample colour image is shown in the Figure 4.3 (a).

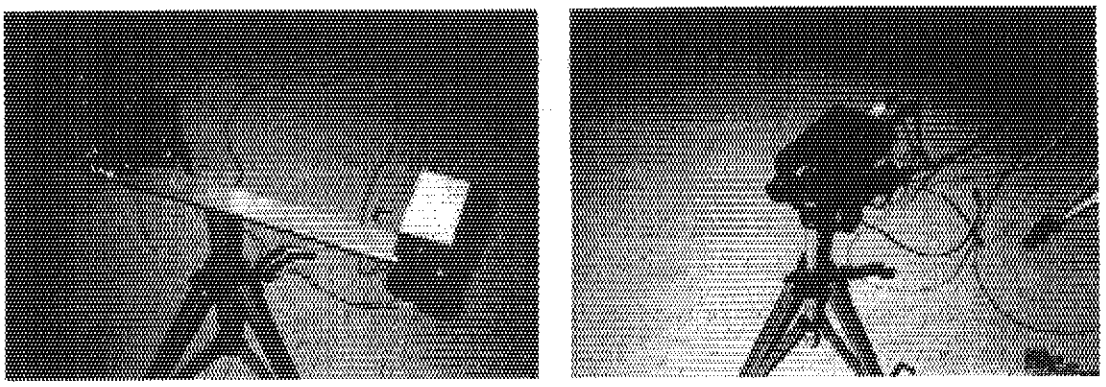

(a) Rangefinder (b) Colour CCD camera

Fig. 2.1 (a) Rangefinder and (b) Colour CCD camera

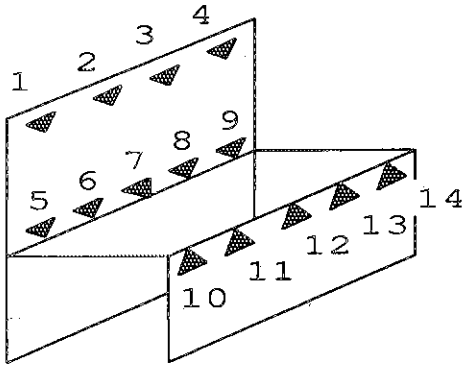


Fig. 2.2 Calibration frame: Black triangle marks are used for calibrating the rangefinder system

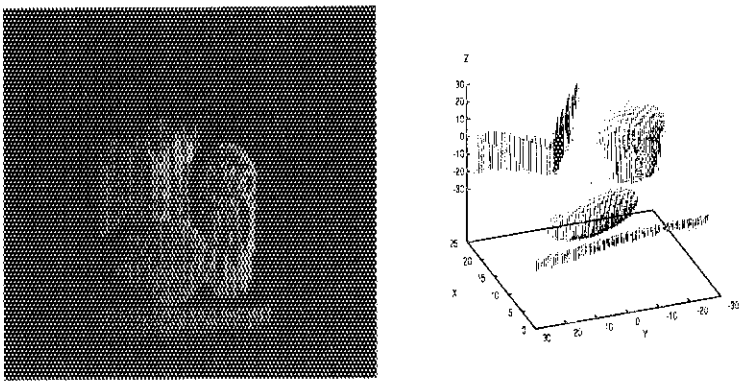

(a) Range image (b) 3D range data

Fig. 2.3 Samples of (a) range image, (b) 3D range data corresponding to the range image and

# 3. Noise Reduction from Range Data

In this section, investigation of noise in range data and the suitable method for reducing noise from range data is described. Since this rangefinder was developed for mobile robot navigation, range data includes much noise while it can be measured quickly. Considering fusion of the range image and the colour image and identification of the surface shape of objects using range data, noise in range data needs to be investigated and reduced. Therefore noise was classified into two different types and each type of noise and several noise reduction methods were investigated.

## 3.1 Definition of Noise Included in Range Data

Noise included in range data could be classified into two different type on the basis of cause for happening noise. One type of noise is lack of range data at pixels in the range image and the other type is the difference from correct range data.

All points of the surface of objects cannot always be measured by the laser-scanning rangefinder. Then several pixels in the range image cannot have range data, that is lack of range data. The vertical light stripe is projected and scanned on the surface of objects by the laser projector and the several reflected light stripes are detected on one identical image by the CCD camera. The range can be obtained only at pixels with the detected reflected light stripes in the image. Although the interval of taking the image of the reflected light stripe is fixed in the CCD camera, the scanning speed of the projected light is variable. Then the interval between reflected stripes in the range image, that is the interval between lines of pixels which detect reflected light stripes, can be determined by the scanning speed. The interval between reflected light stripes also depends on the distance of the surface of objects from the projector. As the distance of the surface of objects from the projector increases, the interval between reflected light stripes in the image becomes wide. Hence the pixels in the interval between reflected light stripes do not have range data in spite of the existence of the surface of objects. That is lack of range data. In this case, an integer 0 is set at the pixel which have no range data.

Generally data which can be measured by a measurement instrument inevitably includes the error which is the difference from the exact range value, that is to say the measurement error. Then range data which is measured by the laser scanning rangefinder includes the measurement error. Since various causes of the measurement error can be considered such as electric noise in the rangefinder system, distortion in the optical system and so on, it is very difficult to specify causes of the error and remove these causes completely. Usually, in data processing field, all causes of noise is regarded as one cause in a whole measurement instrument and so measurement results is investigated to find the characteristic of included noise and to reduce the noise. In this project, reduction of noise due to the measurement error was tried by applying methods of general data processings.

In Figure 3.1, the range image and 3D range data of the plane board of the calibration frame are shown to check included noise.

### 3.2 Supplement of Lack of Range Data

As describing in the previous section, the range image has pixels which lack range data and is set an integer value 0. It is necessary to investigate how these pixels are included in the range image which is obtained by the laser-scanning rangefinder for supplementing lack of range data in such pixels. In order to investigate lack of range data in the range image, the binary range image was generated from the original range image. In the binary range image, the white pixel has range data and the black pixel has no range data. The binary range images of the plane board of the calibration frame which was set at various distances are shown in Figure 3.2.

According to Figure 3.2, the interval between white pixels is almost one pixel and so the eight nearest neighbor around one black pixel in the interval may include six white pixels at least. Then the median filter, which is a window operator, can be utilized for supplementing black pixel between white pixels because the range value at the central pixel in the window of the median filter is replaced with the median value in the window. Hence to apply the $3 \times 3$ median filter to only black pixels is effective for supplementing lack of range data of pixels in the range image. In Figure 3.2, the binary range image which is obtained after applying the $3 \times 3$ median filter to only black pixels iteratively are also shown. According to these figures, it is found that lack of range data on the surface of the plane in the range image is supplemented.

### 3.3 Reduction of Noise Due to Measurement Error

To investigate noise due to the measurement error in the range data, the analytical plane equation was fitted to range data and the histogram of the deviation from the analytical plane equation was generated. Then the shape of the deviation histogram and the standard deviation of this histogram was used for checking the effect of noise reduction. First, the influence of supplementing lack of range data on the shape of range data was checked using the deviation histogram. In Figure 3.3, the deviation histograms of original range data and of range data after supplementing lack of range data are shown. Since the remarkable difference between these two histograms cannot be found in this figure, it is supposed that supplement of lack of range data does not influence distance values of original range data. As for the measurement error noise, three methods that are the median filter[3], the arithmetic mean filter[4] and the accumulative average method[5] were tried to reduce noise due to the measurement error.

The median filter can remove salt-and-pepper noise while the spatial details such as the edge in the image is preserved. This is the reason why the median filter worked effectively for supplementing lack of range data as describing in the previous section. In this project, four types of the median filter whose size are $3 \times 3$, $5 \times 5$, $7 \times 7$ and $9 \times 9$ respectively were tried to reduce noise in the range image. Each median filter was applied to all pixels in the range image iteratively. The histograms of the deviation from the analytical plane equation for range data obtained after reduction of noise using the median filter are shown in Figure 3.4, 3.5 and 3.6.

The arithmetic mean filter is a no-weighted average window operator. The average of all range data within the window operator is calculated and range data at the center of the window is replaced by the calculated average value. Then the spatial details such as the edge become dull as the window size is large. The arithmetic mean filters whose sizes are $3 \times 3$, $5 \times 5$, $7 \times 7$

and 9 × 9 respectively were tried to check the effect for reduction of noise as well as the median filter. Each arithmetic mean filter was applied to the range image iteratively. The histograms of the deviation from the analytical plane equation for range data obtained after reduction of noise using the arithmetic mean filter are shown in Figure 3.7, 3.8 and 3.9.

The accumulative average is a time sequential method while above two methods, the median filter and the arithmetic mean filter, are spatial methods. In the accumulative average method, since range data in pixels with identical coordinates in several different range images of one scene are averaged, noise which happens randomly can be reduced. Then the effect of reduction of noise using the accumulative average method increases as the number of range images which are used for averaging increases. Five, 10, 20 and 30 range images were used for reducing noise. The histograms of the deviation from the analytical plane equation for range data obtained after reduction of noise by the accumulative average method are shown in Figure 3.10.

According to the investigation described above, the arithmetic mean filter is the best way for reducing noise due to the measurement error among these methods such as the median filter, the arithmetic mean filter and the accumulative average method. Since the accumulative average requires a number of range images, it takes much time to detect many range images and to process them. Therefore this method is not suitable for the application of the recognition system to a mobile robot. Since the median filter preserves spatial details such as the edge, it does not change the surface shape of solids in the range image. However the step edge due to the discretization of range and the measurement error are emphasized rather than they are reduced. Hence the arithmetic mean filter method was adopted for reducing noise due to the measurement error. According to Figure 3.7, 3.8 and 3.9, the standard deviation of the deviation histogram for range data obtained by applying the 9 × 9 arithmetic mean filter one time is minimum. Therefore the 9 × 9 arithmetic mean filter is applied one time on the range image for reducing noise.

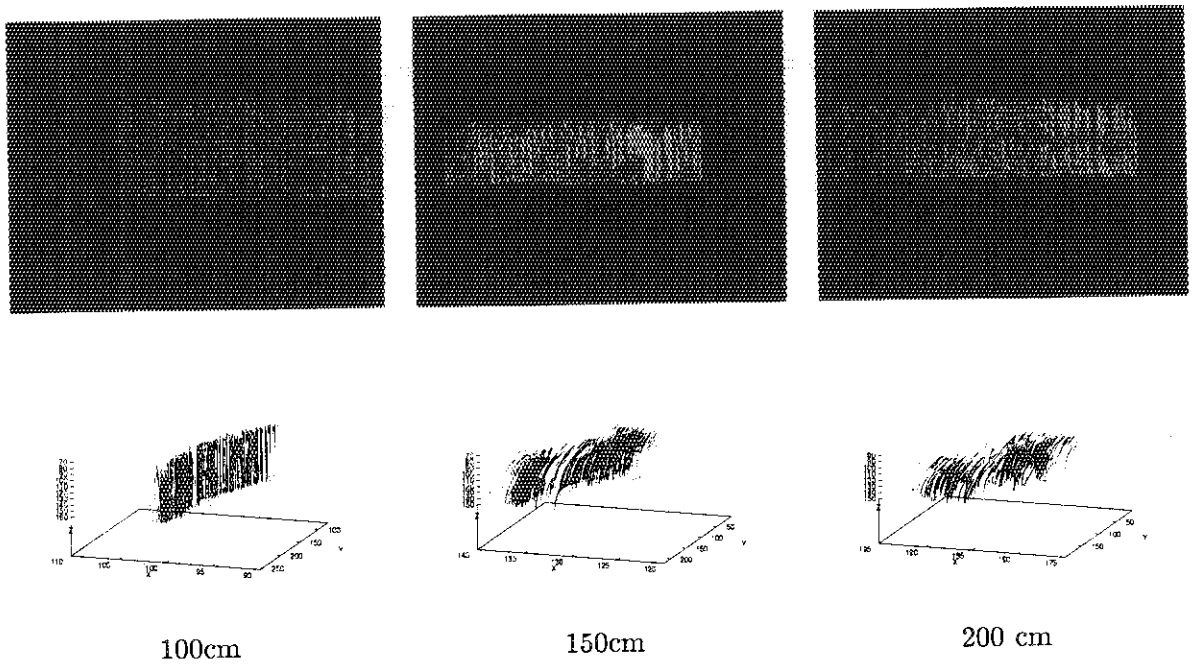

100cm 150cm 200 cm

Fig. 3.1 Range images of the plane board of the calibration frame and their 3D representation:Range is represented by the gray level in the range image. The Black pixel means lack of range data.

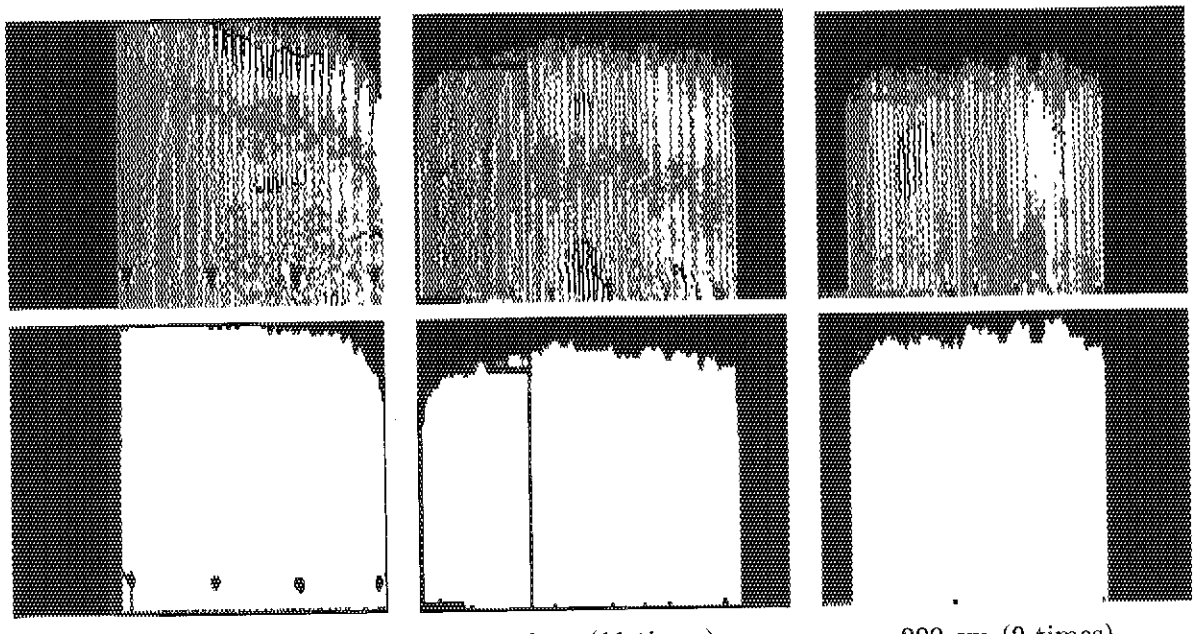

100cm (13 times) 150cm (11 times) 200 cm (9 times)

Fig. 3.2 Binary range image: The images in the top row are binary images before supplementing lack of range data. The images in the bottom row are after supplementing lack of range data. The number in parentheses means frequency of iteration.

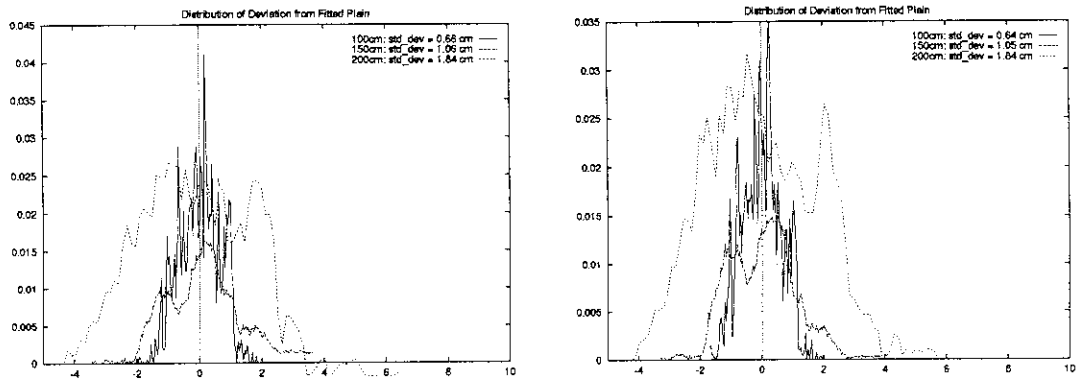


(a) (b)

Fig. 3.3 (a) Histogram of the deviation for original range data, (b) Histogram of the deviation for range data obtained after supplementing lack of range data

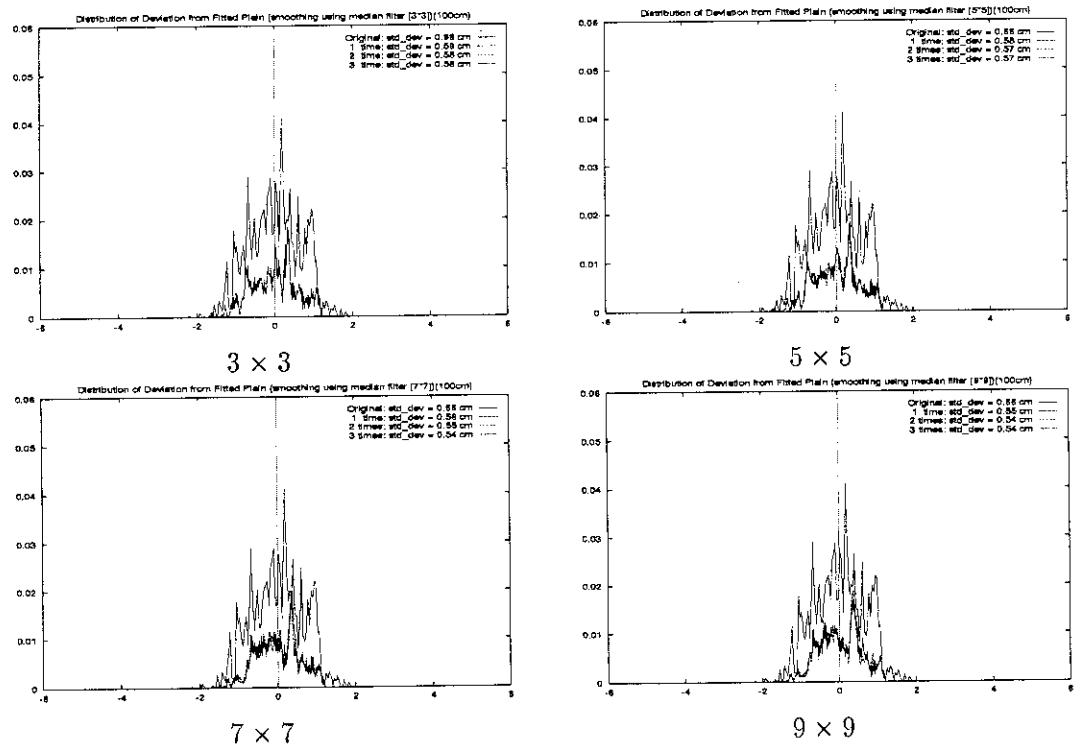


3 × 3 5 × 5

7 × 7 9 × 9

Fig. 3.4 Histogram of the deviation for range data obtained after reducing measurement noise using the median filter (100cm)

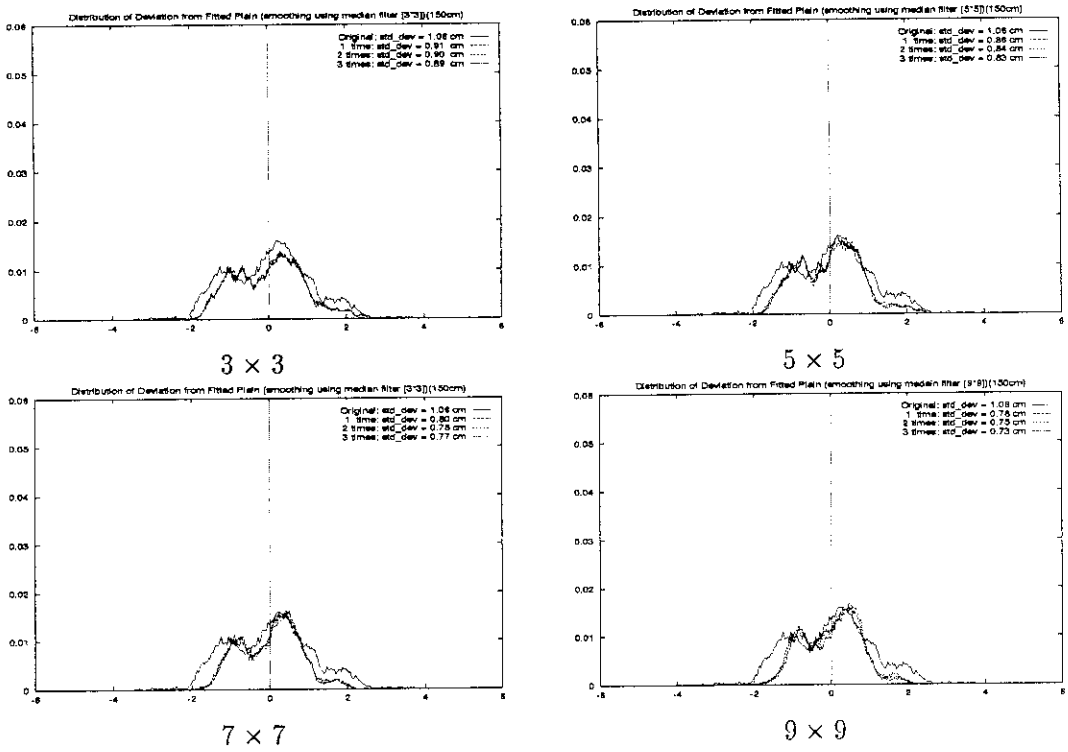


Fig. 3.5 Histogram of the deviation for range data obtained after reducing measurement noise using the median filter (150cm)

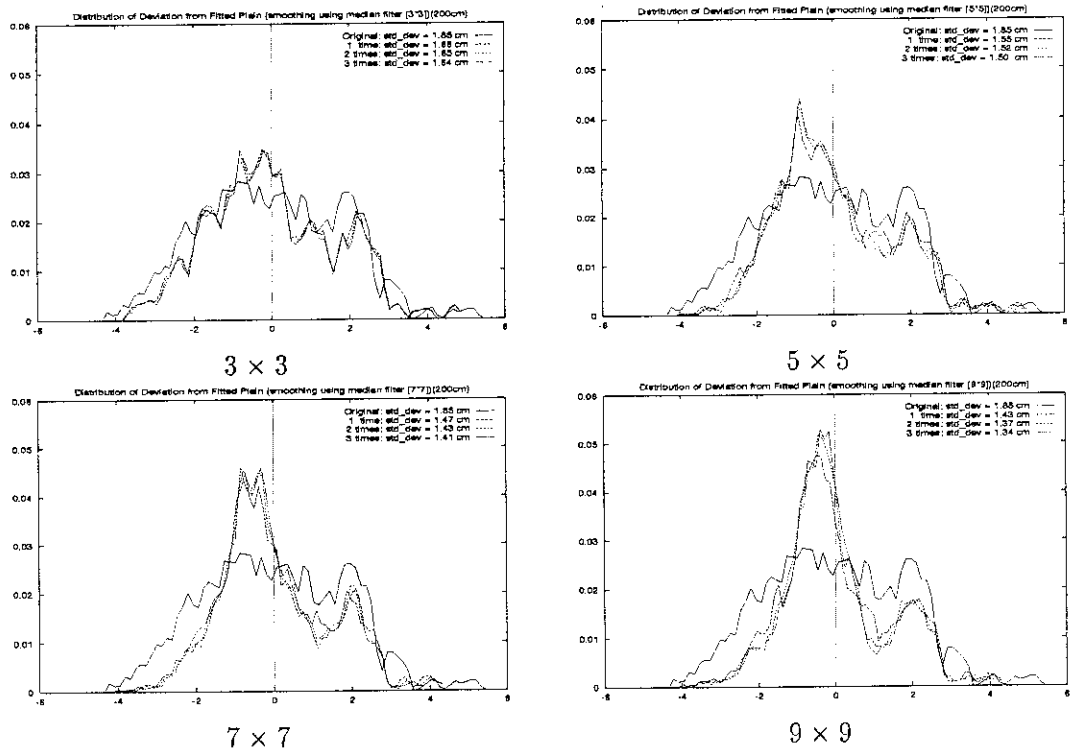


Fig. 3.6 Histogram of the deviation for range data obtained after reducing measurement noise using the median filter (200cm)

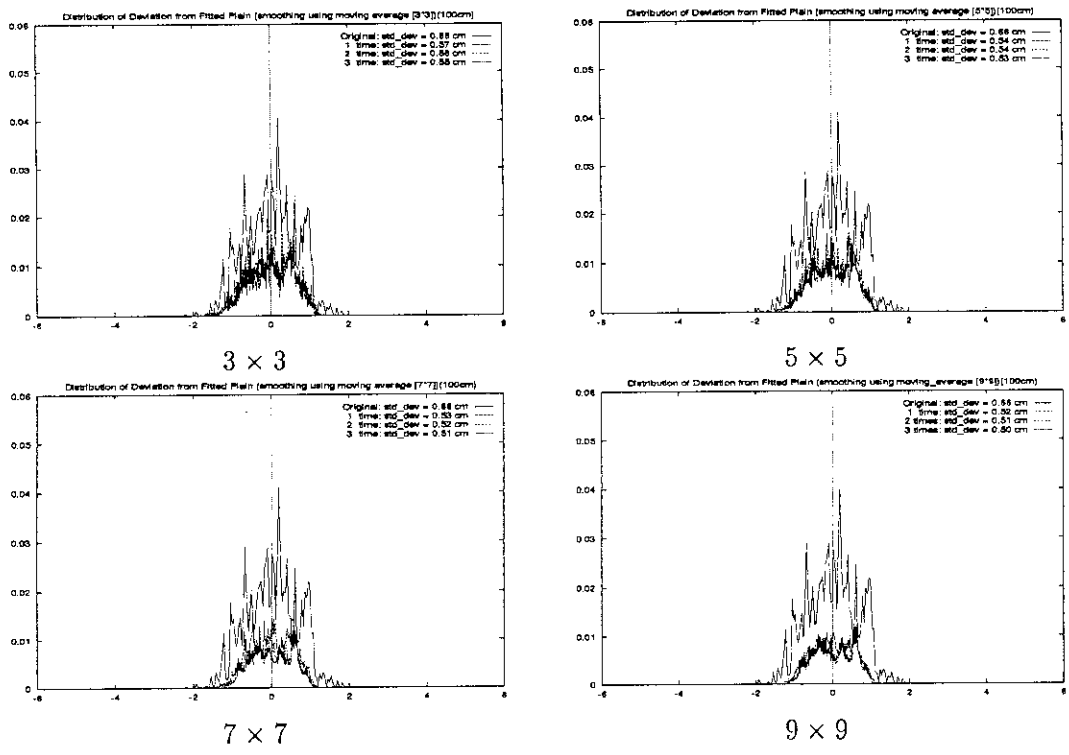


Fig. 3.7 Histogram of the deviation for range data obtained after reducing measurement noise using the arithmetic average method (100cm)

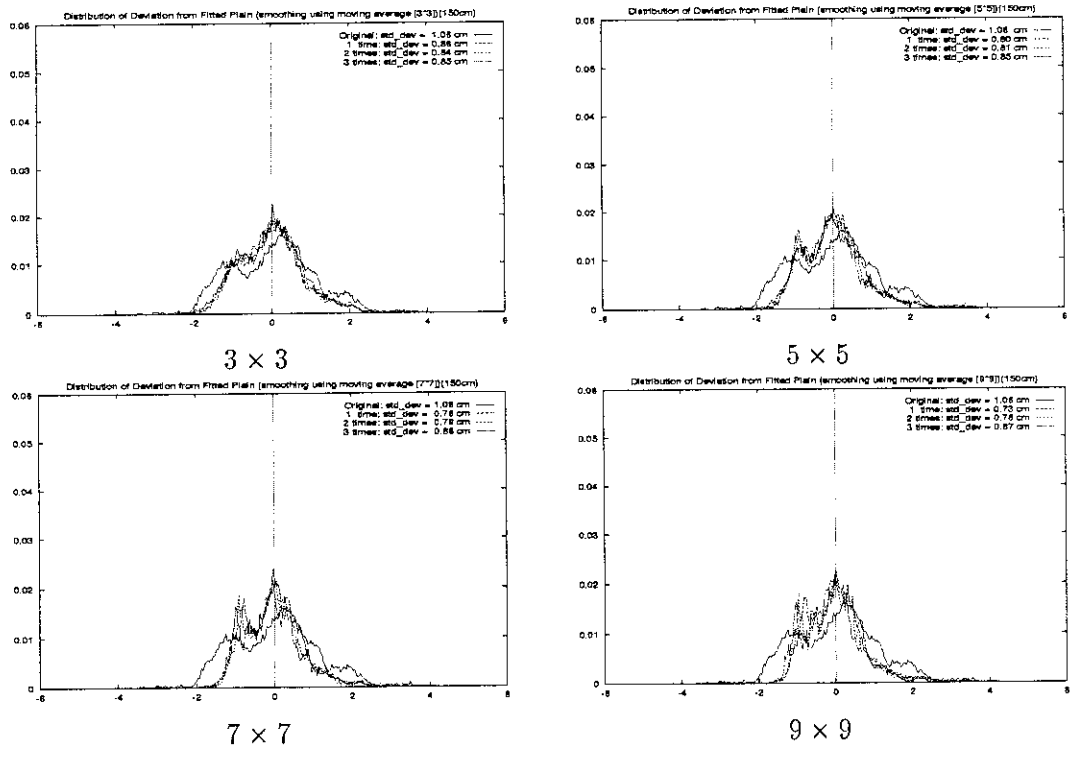


Fig. 3.8 Histogram of the deviation for range data obtained after reducing measurement noise using the arithmetic average method (150cm)

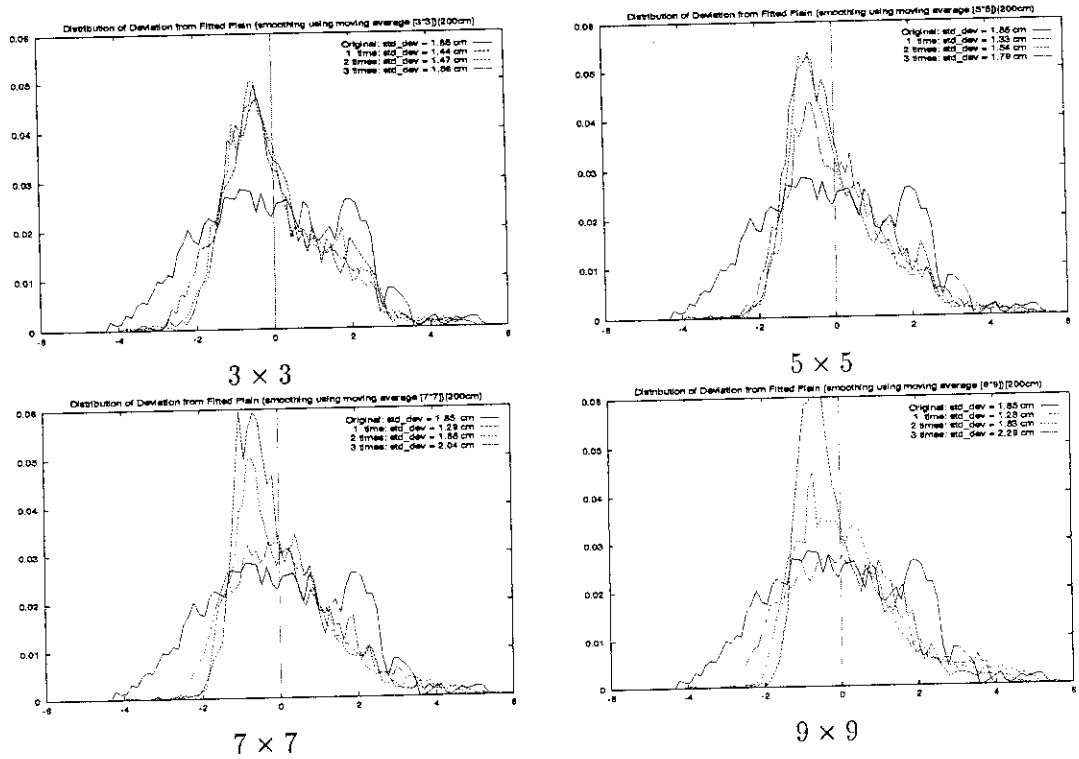


Fig. 3.9 Histogram of the deviation for range data obtained after reducing measurement noise using the arithmetic average method (200cm)

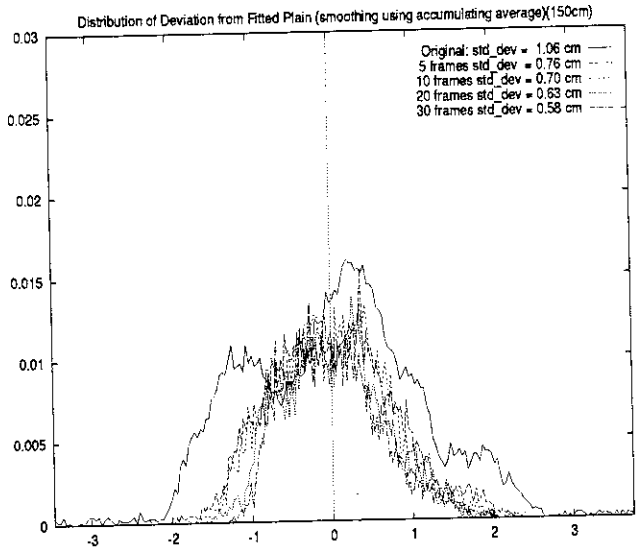


Fig. 3.10 Histogram of the deviation for range data obtained after reducing noise using the accumulative average method

# 4. Colour Image Segmentation using Range and Colour Information

In this section, segmentation of the colour image to each region of geometrically shaped solids using range and colour information is mainly described. The colour image was segmented into regions comparatively easily and effectively by fusion of colour and range information. The image obtained after segmentation is used as a filter for extracting range data of each solid.

## 4.1 Outline of Fusion of Colour and Range Information

The flow of fusion of colour and range information in the developed program is shown in Figure 4.1. As drawing in this figure, the colour image and range data are transformed into various forms which are expedient for processes in each step and are fused. As for the range data, lack of range data in the range image is supplemented so that the intermediate range image is obtained. Using this intermediate range image, the binary range image and the smoothed range image are generated. The smoothed range image is transformed into range data represented in the 3-dimensional coordinate system, that is 3D range data. The 3D range data is used for calculating the normal vector on the surface of solids and for identifying the surface shape of solids by fitting analytical surface equations. As for the colour image, its background is eliminated using the binary range image to obtain the clipped colour image. The labeled image is generated from the clipped colour image using colour information and the relabeled image is generated from the labeled image using normal vectors on the surface of solids which are obtained from 3D range data. The relabeled image is used for extracting range data corresponding the surface of each geometrically shaped solid. The detail of each process is described in following sections.

## 4.2 Background Elimination from Colour Image

Elimination of the background from the colour image is one realization of fusion of colour and range information. The range image is utilized as one representation of range information in this part. However range information itself is not used. The range image is used as a filter for clipping object regions out of the colour image. That is the binary range image as described in the section 3.2. The binary range image, the corresponding original colour image and the clipped colour image obtained by eliminating the background are shown in Figure 4.3. The colour image was manually overlaid with the colour image in this program.

## 4.3 Colour Image Segmentation Using Hue and Saturation

### 4.3.1 Definition of HS distribution

Since it is assumed that each geometrically shaped solid has its own unique colour in this project, the clipped colour image can be segmented into each region which has one geometrically

shaped solid by segmenting the clipped colour image using colour information. Therefore the labeled image in which each region of one geometrically shaped solid is labeled can be obtained by segmenting the clipped colour image using colour information.

Among many types of representation of colour information, Munsell colour system[7], that is H(hue), S(saturation), I(intensity) representation, was adopted as a colour representation for segmenting the colour image because information of colour attribution can be almost separated from intensity information in this representation so that colour information except intensity information can be handled under a certain condition. In Munsell colour system, hue is represented by the angle of the radial direction in the unit circle and saturation by the length of the radius of this circle, which is normalized, and intensity by the length of the perpendicular direction which pierces the center of this circle and is also normalized. Therefore it is possible to handle colour attribution which is included in hue and saturation by projecting points in HSI space onto an unit circle. In Figure 4.2, the distribution on the unit circle which was obtained from the sample colour image in Figure 4.3 (a) by this way is shown. This distribution is the Hue-Saturation distribution, that is the HS distribution.

### 4.3.2 Relation between colour in the colour image and the cluster in HS distribution

Each cluster in HS distribution in Figure 4.2 corresponds to each colour in the colour image. Therefore the correspondence between the cluster and colour of the solid in the colour image was investigated. The various images of coloured solids were taken by the colour CCD camera and the colour information, which is represented in the RGB colour system, in each pixel of the colour image was transformed to HSI colour system so that HS distribution is generated. The colour images are shown in the Figure 4.6, 4.7 and 4.8, the corresponding HS distribution in the Figure 4.10, 4.11 and 4.12. According to these colour images and HS distributions in the figure, it is found that there is the obvious correspondence between colour in the colour image and the cluster in HS distribution and that the size and the shape of the cluster does not change so remarkably as the size of the region including the coloured solid in the colour image changes. It is also found that the arrangement of coloured solids dose not influence the shape and the size of the cluster in HS distribution unless the kinds of colour of solids in the image are changed. Therefore regions in the colour image can be segmented by classifying clusters in HS distribution.

Each cluster in HS distribution corresponds to colour in the colour image. However the cluster shape in HS distribution depends on the illumination condition around objects. In the case of being dark around objects, the cluster shape become vague and the edge of the cluster become dull. In order to investigate this phenomenon in HS distribution, the colour image of one scene was taken under several illumination conditions and the corresponding HS distribution was generated. The results of this experiment are shown in Figure 4.5 and 4.9. Since the illumination condition were not investigated quantitatively, however, optimal brightness or the upper and lower limitation cannot be specified clearly. Therefore the colour image with clear clusters in HS distribution was used in this project.

### 4.3.3 Colour Image Segmentation

In previous sections, it was found that the colour image might be segmented by classifying clusters in HS distribution of the colour image. Then the Voronoi diagram[8] was used as the

classification method for clusters in HS distribution of the colour image. The way for making the Voronoi diagram is as follows:

(1) Making the HS histogram by discretizing HS distribution,

(2) Searching in the HS histogram for local maxima that are generators for each cell of the Voronoi diagram,

(3) Classifying all points in the HS histogram into the cell with their nearest generator in the Voronoi diagram.

Each cell in the Voronoi diagram which is generated by the above way almost includes each cluster in the HS distribution. Therefore the points in one cell correspond to regions with same colour in the colour image.

In the case of practical segmentation of the colour image, the colour image is divided into several squares and the above segmentation method is applied to the HS distribution for each square. Because a few number of pixels is in each square, the computation for generating the Voronoi diagram is not so expensive. The colour image can be also segmented finely into one colour regions by dividing the colour image into squares. In Figure 4.4 (a), (b) and (c), the divided colour image, one sample square and its HS distribution are shown. In Figure 4.4 (d), (e), the HS histogram which was used for dividing the sample square and the Voronoi diagram corresponding to this HS histogram are shown.

After segmenting squares, all squares are unified to one segmented colour image and small regions whose area is less than a certain threshold value are merged to the nearest large region. In this case, the measure of the distance between regions in the segmented colour image is similarity of the colour attribution in the HS distribution space. In addition, each region in the segmented colour image is labeled in the numerical order to make the labeled image. In Figure 4.4 (f), the obtained labeled image is shown. The label is represented by the gray level in this figure.

Considering to extract range data which corresponds to each geometrically shaped solid using the labeled image as a filter and to fit the analytical curved surface equation to extracted range data, the analytical equation of the curved surface is inevitably fitted to the range data corresponding to the solid with plane surfaces such as a rectangular solid and a pyramid in case that the roof edge of such solids appears in the image. Therefore the region of solids which are formed by plane surfaces in the labeled image had better be segmented into regions of the plane of such solids.

## 4.4 Colour Image Resegmentation Using the Normal Vector

As describing in the previous section, the labeled image in which regions with same colour are labeled in the numerical order is generated using colour information. However the range data of the solid with plane surfaces which is extracted by using the labeled image as a filter is not useful to distinguish between the curved surface and the plane surfaces which make the roof edge by fitting the analytical surface equation. Hence it is necessary to resegment the region for the solid with plane surfaces into regions of the plane. The normal vector at each point on the plane surfaces which make the roof edge was used for segmenting the region of the solid with plane

surfaces because the direction of the normal vectors on the plane surfaces changes at the roof edge abruptly while the direction of the normal vectors on the curved surface changes at every point continuously. The orientation distribution of the normal vector on the unit sphere for the surface of each region in the labeled image(Figure 4.4 (f)) is shown in Figure 4.13. According to this figure, it is found that there are two separate large clusters on the unit sphere for the surface of the rectangular solid and there is one large cluster for other curved surfaces. Hence the difference of change in the orientation of the normal vector is available for distinguishing between the roof edge which is made by plane surfaces and the curved surface.

In order to segment the region of the plane surfaces which make the roof edge into regions of the plane, the orientation histogram of the normal vector on the unit sphere was used. This is an application of the needle diagram[9]. The way to make the orientation histogram of the normal vector is as follows:

(1) Calculating the normal vector on the surface in each region in the labeled image,

(2) Putting the tail of all normal vector in each region on the center of the unit sphere for making the orientation distribution,

(3) Dividing the surface of the unit sphere into regions with the same area by using the geodesic dome[10](Figure 4.14 (a)),

(4) Counting the number of the normal vector in the same region on the unit sphere,

where the region on the unit sphere is specified by the vertex vector of the geodesic dome. Then the orientation histogram is generated on the surface of the unit sphere. After finding local maxima in the orientation histogram of the normal vector, the Voronoi diagram is made on this divided surface of the unit sphere as well as the case of making the Voronoi diagram for the HS histogram. Using this Voronoi diagram on the unit sphere, the regions in the labeled image are segmented again so that the relabeled image is generated. In this case, the small region whose area is less than the provided threshold value is eliminated from the relabeled image. In other words, the part of the surface whose normal vectors are included in the cell with a few normal vector on the unit sphere is removed from the relabeled image which is generated after segmentation using the normal vector. Because the direction of normal vectors in the small region is different from that of normal vectors in the large region, the range data which is used for calculating the normal vector in such a small region are not adequate for fitting the analytical surface equation. Therefore the part of the region in the labeled image which extracts such range data is removed rather than being merged to other regions. In Figure 4.14 (b), the relabeled image was obtained by segmenting the labeled image (Figure 4.4 (f)) using the normal vector is shown. In this figure, spots in each region are caused by removing small regions. This relabeled image is used for extracting range data of the surface of each geometrically shaped solid.

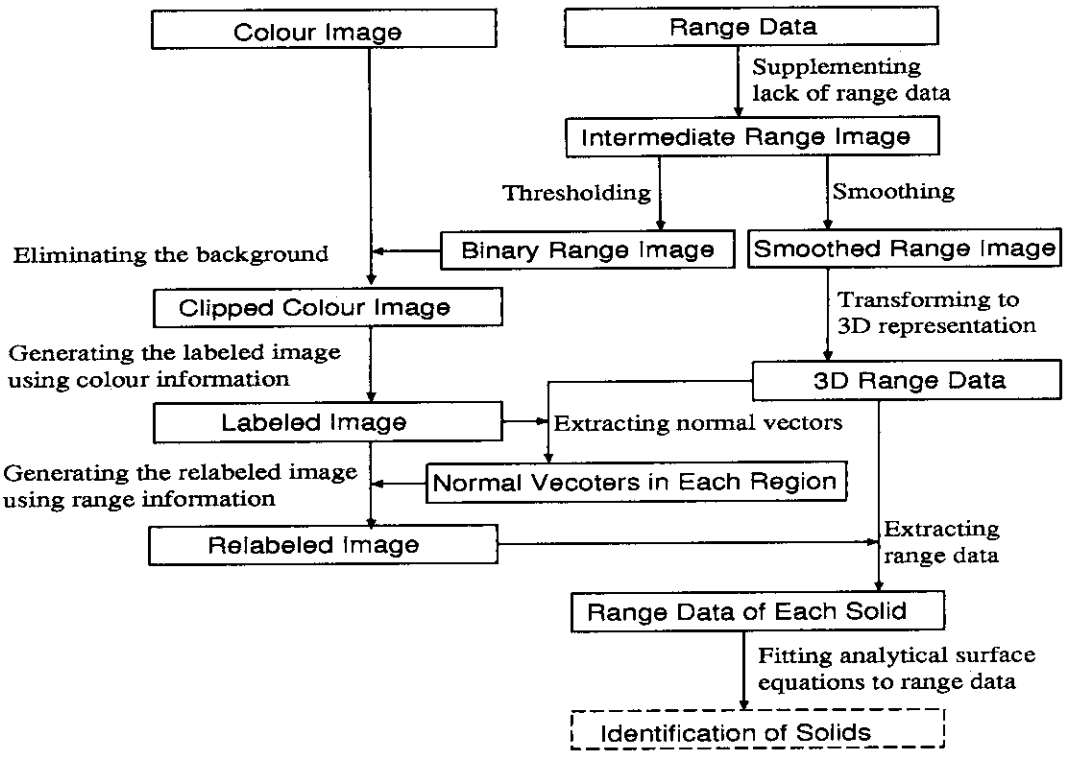


Fig. 4.1 Flow for fusion of colour and range information

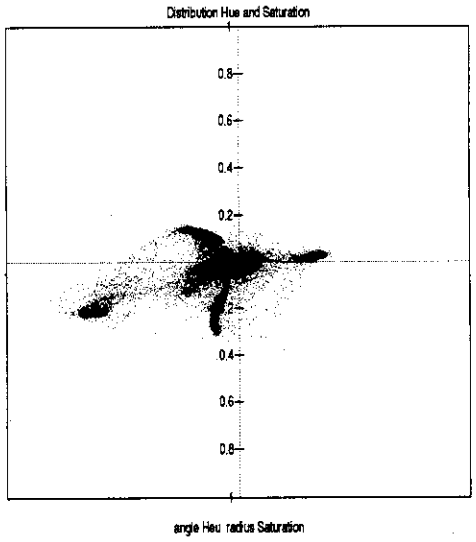


Fig. 4.2 HS distribution for sample colour image in figure 2.3

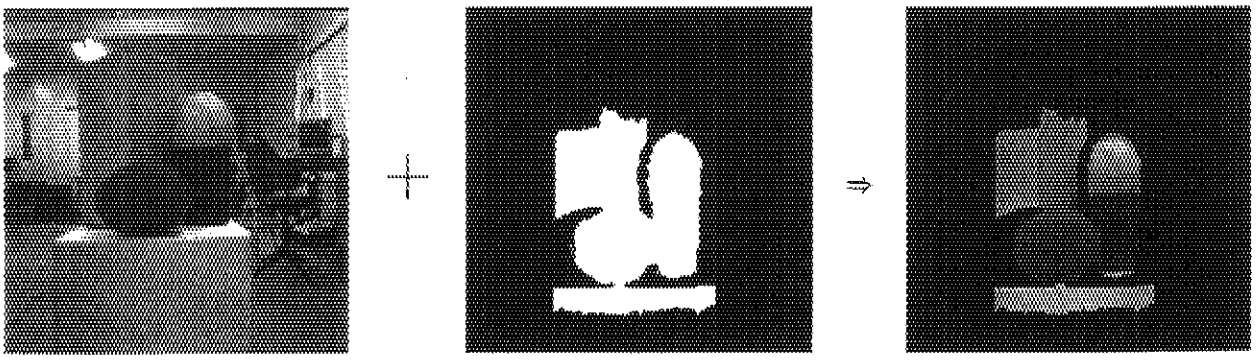

(a) (b) (c)

Fig. 4.3 Eliminating the background from the original colour image using the binary range image: (a) Original colour image, (b) Binary range image and (c) Image obtained by eliminating background

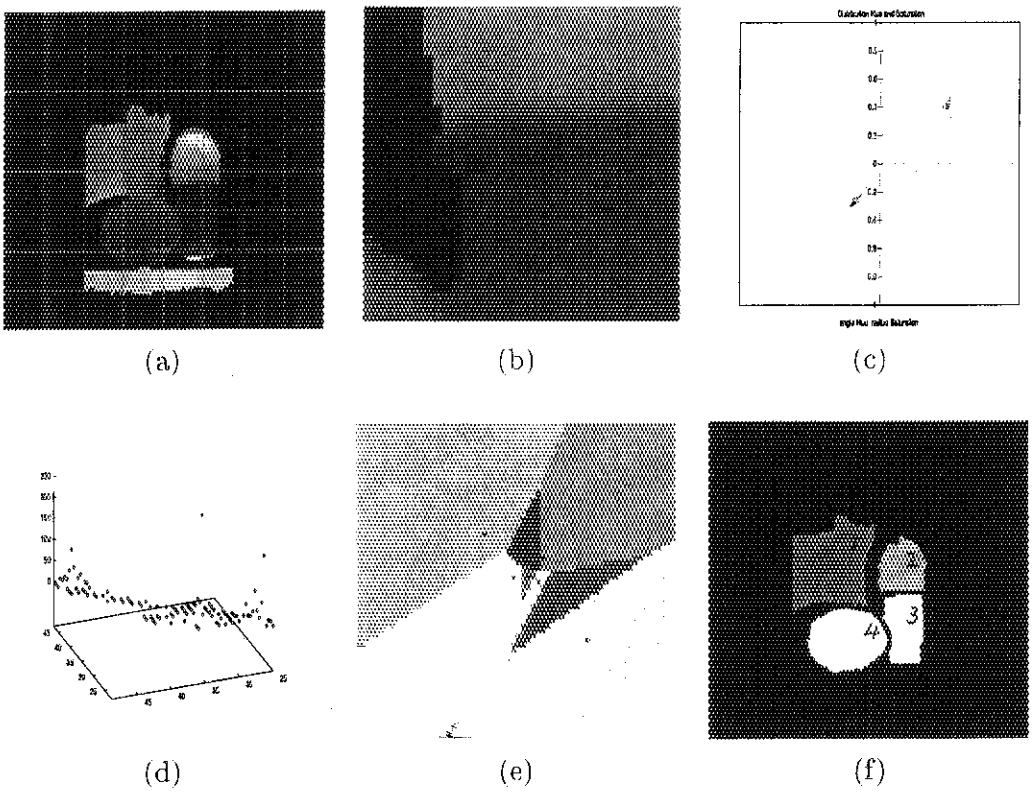

(a) (b) (c)

(d) (e) (f)

Fig. 4.4 (a) The divided colour image into squares, (b) the sample square corresponding to square encircled by the red line in (a), (c) the HS distribution of the sample square, (d) the HS histogram of the sample square (Black points represent local maxima.), (e) the Voronoi diagram of the sample square (Green points means generators.) and (f) the obtained labeled image.

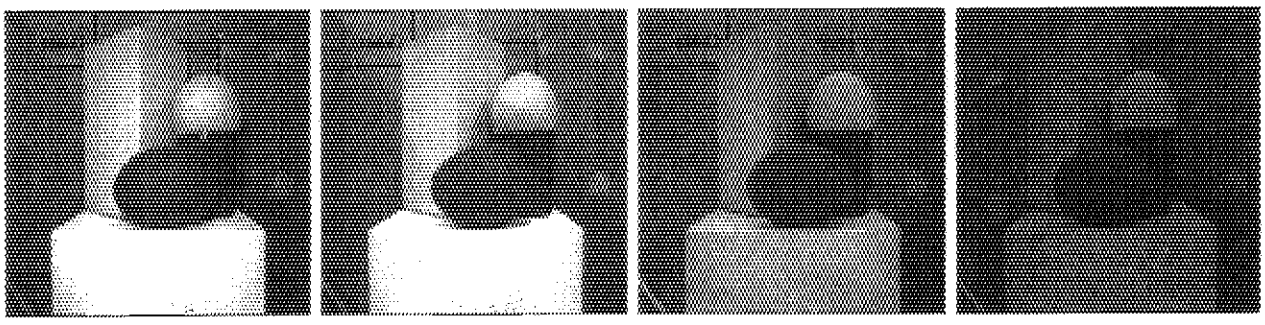

Fig. 4.5 The colour image (1) (For checking dependence on lightness)

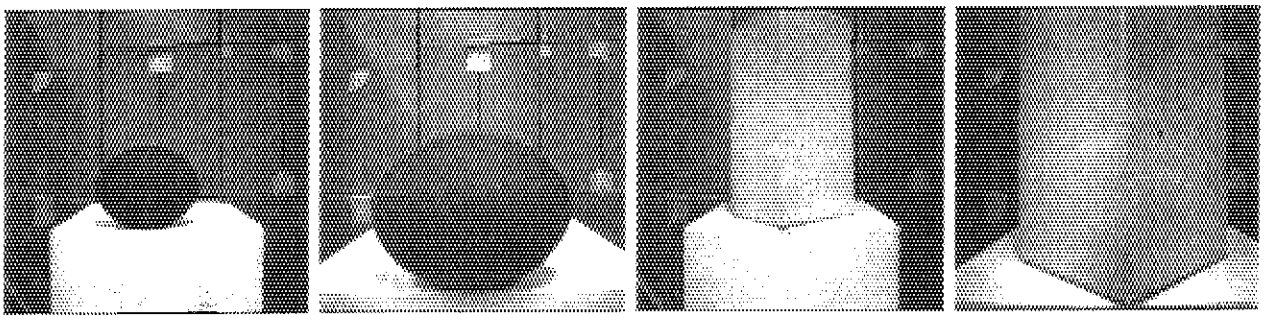

Fig. 4.6 The colour image (2) (For checking dependence on the size of the occupied region by the coloured solid in the color image)

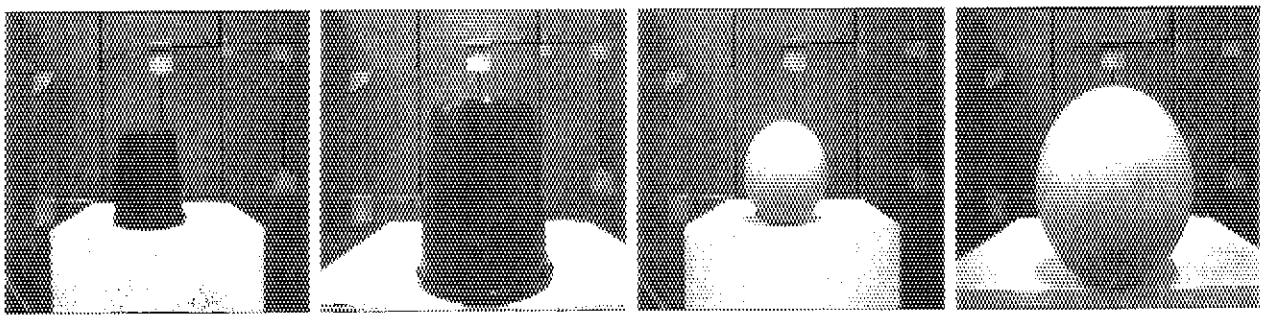

Fig. 4.7 The colour image (3) (For checking dependence on the size of the occupied region by the coloured solid in the color image)

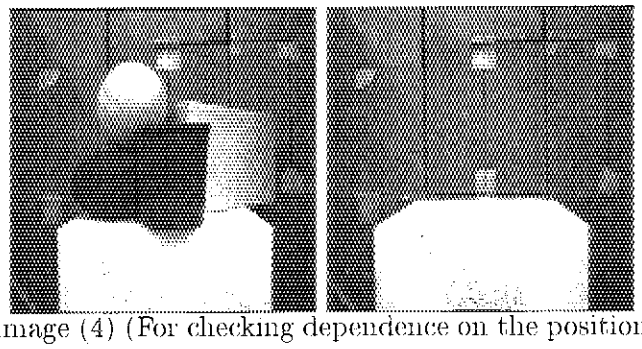

Fig. 4.8 The colour image (4) (For checking dependence on the position of the occupied region by coloured solids in the color image

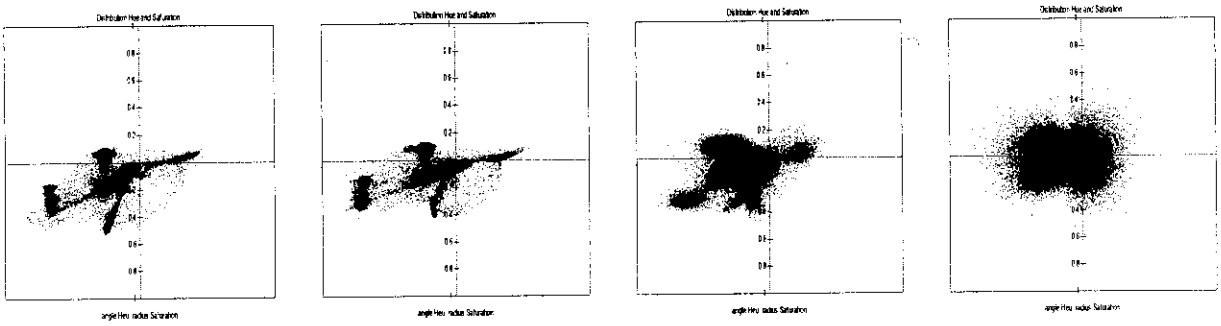

Fig. 4.9 The distribution of hue and saturation (1) (For checking dependence on lightness)

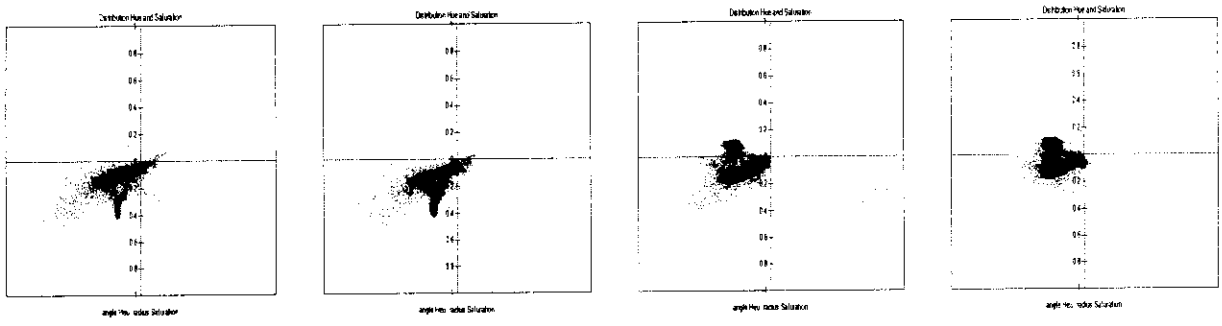

Fig. 4.10 The distribution of hue and saturation (2) (For checking dependence on the size of the occupied region by the coloured solid in the color image)

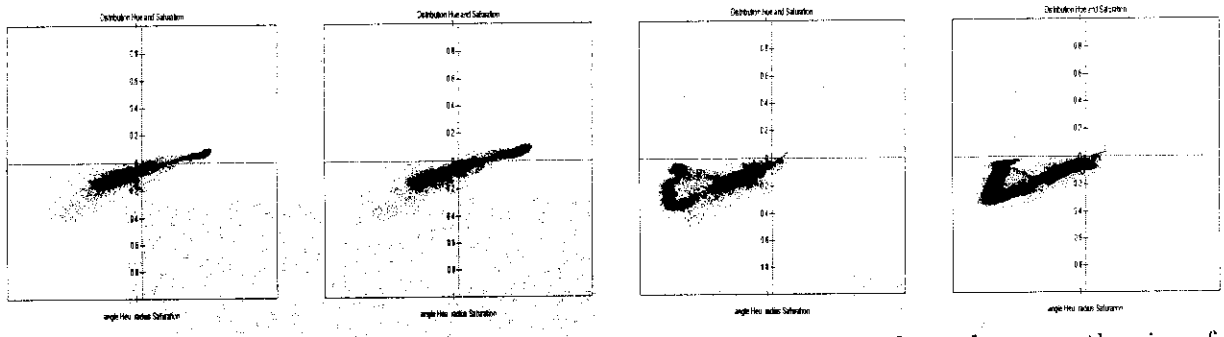

Fig. 4.11 The distribution of hue and saturation (3) (For checking dependence on the size of the occupied region by the coloured solid in the color image)

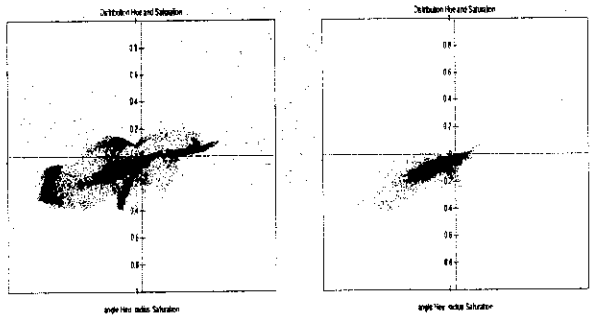

Fig. 4.12 The distribution of hue and saturation (4) (For checking dependence on the position of the occupied region by coloured solids in the color image)

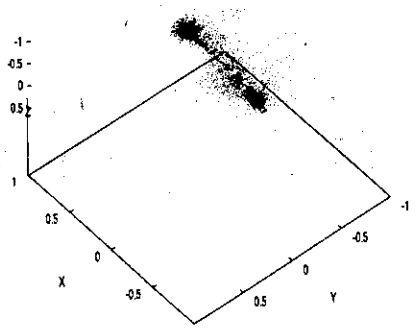

Region 1

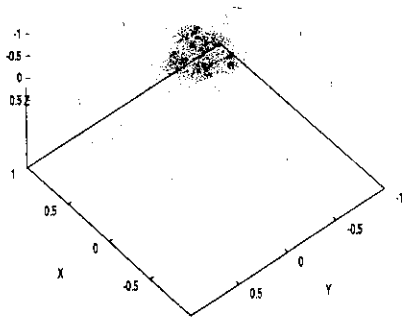

Region 2

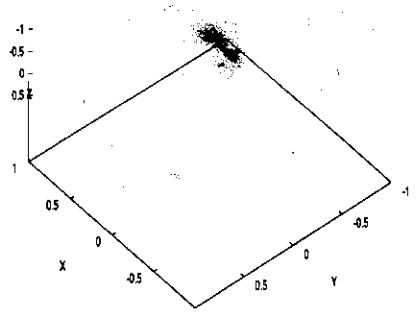

Region 3

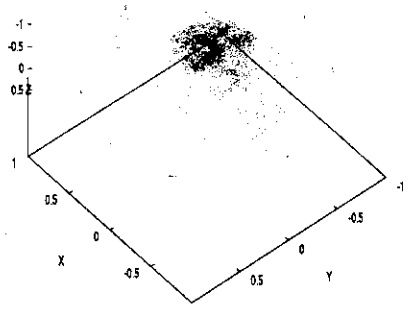

Region 4

Fig. 4.13 Orientation distribution of the normal vector for the surface of each region in the label image

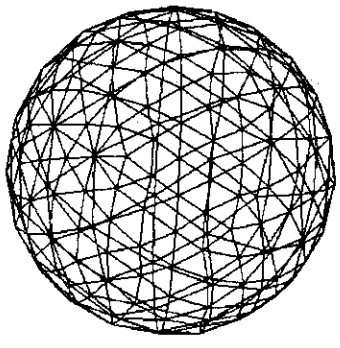

(a) Geodesic dome

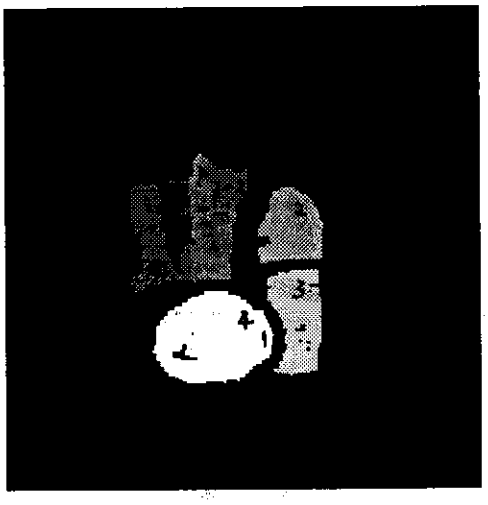

(b) Relabeled image

Fig. 4.14 (a) The geodesic dome and (b) the relabel image

# 5. Identification of Geometrically Shaped Solids

Each geometrically shaped solid is identified by means of fitting the analytical equation of the curved surface to range data which is extracted using the relabeled image obtained in the previous section. In Figure 5.1, the concept of identification of geometrically shaped solids is shown. As being drawn in this figure, the plane surface and the curved surface are distinguished using the eigenvalue of the covariance matrix[6] of the distribution of range data in the 3-dimensional coordinate system. After distinguishing between the plane surface and the curved surface, the analytical equation of the plane surface are fitted to range data of the plane surface and the analytical equation of the curved surface is fitted to the curved surface. Then the surface of each geometrically shaped solid will be identified by using coefficients of each analytical surface equation.

In Figure 5.2, sample colour images of various solids are shown. In Figure 5.3 to 5.16, the relabel images of the colour images in Figure 5.2, their extracted range data and their several data are shown. The data in these figures includes eigenvalues of the covariance matrix and coefficients of the fitted analytical surface equation. As being printed in this figure, when the minimum eigenvalue among three eigenvalues of the covariance matrix of the distribution of extracted range data is less than a certain threshold which is 0.1 $cm^2$ at present, the corresponding region of the surface is classified into the plane surface. The threshold value depends on noise included in range data. In the opposite case, the surface is classified into the curved surface. For the curved surface, coefficients of the standard form of the quadratic curved surface equation,

$$ax^2 + by^2 + cz^2 + dx + ey + fz + g = 0, \tag{5.1}$$

which is obtained by transforming the coordinate system for the general form of the quadratic equation, are printed. For the plane surface, components of the normal vector of the plane surface are printed. The components of the normal vector of the plane surface are coefficients of the liner term of the plane surface equation.

According to coefficients of the quadratic curved surface equation, the side surface of the cone can be distinguished from the surface of other solids because the absolute value of the constant term of the quadratic curved surface equation which is fitted to range data of the side surface of the cone is negative while that for other solids with the curved surfaces is positive. Identification of the surface of the cylinder, the sphere and the ellipsoid may be possible by using coefficients of the quadratic term of the curved surface equation though that has not been considered. The possibility of this identification may depend on accuracy of range data.

It may be difficult to identify solids which are formed by plane surfaces such as the rectangular solid and the pyramid only using the normal vector of the plane surface. It is impossible to distinguish between the rectangular solid and the pyramid when the part of the surface of such solids is only visible. Therefore the position, the orientation, the area of the plane surface and the relation among plane surfaces such as connectivity need to be checked using range data and colour image. After that, it may be possible to identify solids which are formed by plane surfaces.

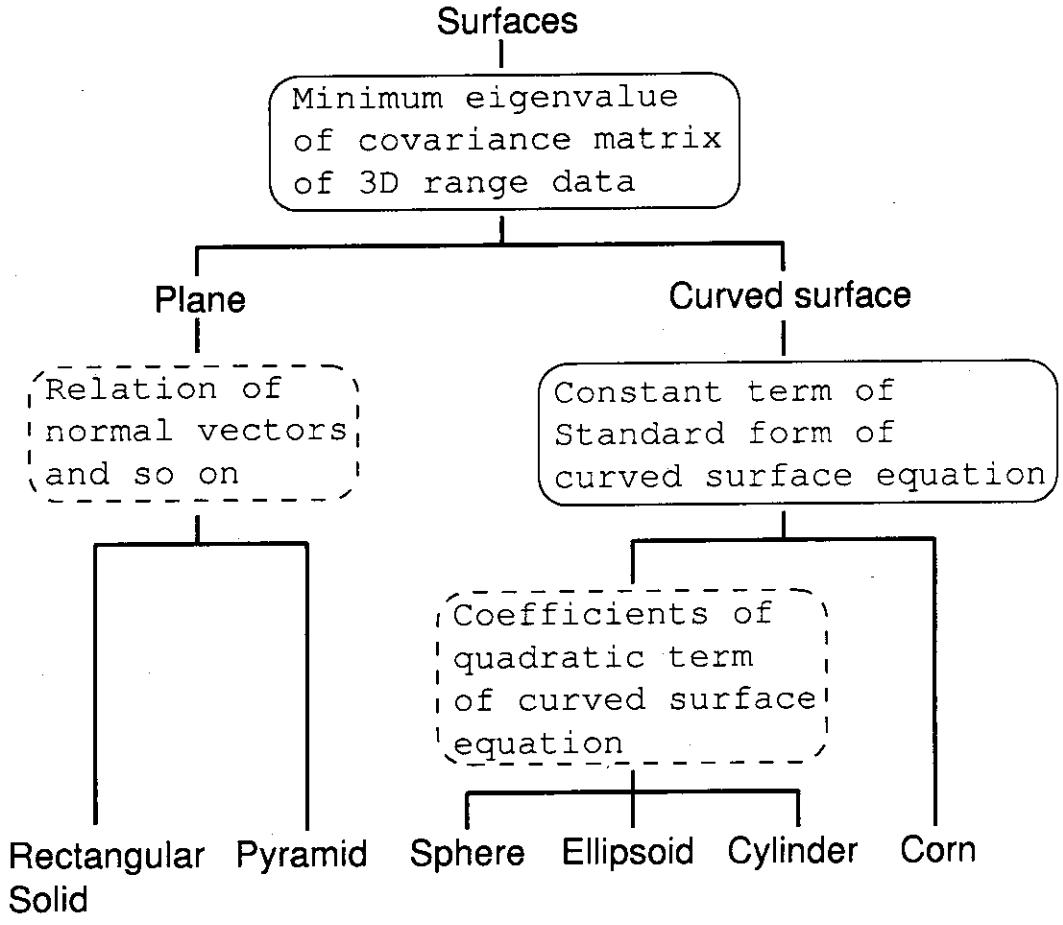


Fig. 5.1 A concept of identification of geometrically shaped solids

Fig. 5.2 Sample color images: (1) A yellow sphere, (2) A large blue cone, (3) A small red cone, (4) A declined small red cone, (5) A standing green cylinder, (6) A laying green cylinder, (7) A red ellipsoid (a), (8) A red ellipsoid (b), (9) A green rectangular solid, (10) A yellow pyramid with three side surfaces, (11) A yellow pyramid with four side surfaces, (12) A declined yellow pyramid with four side surfaces, (13) A combination of various solids

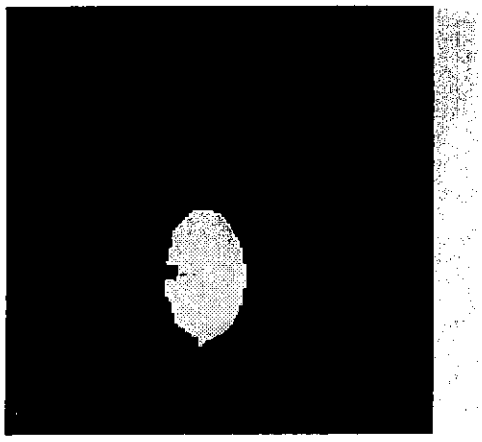

Segmented Colour Image

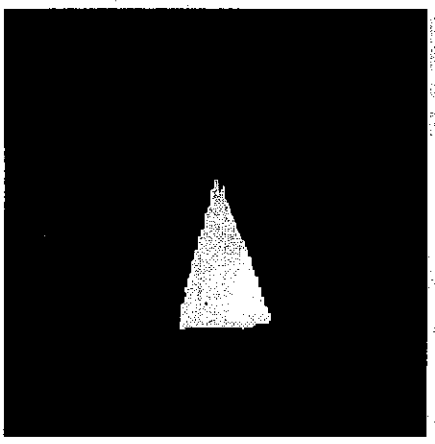

Segmented Colour Image

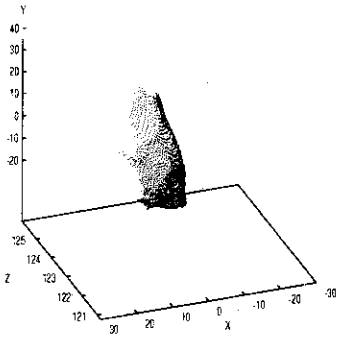

Extracted Range Data

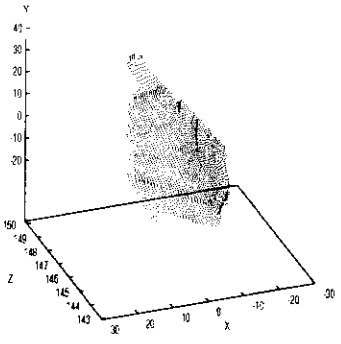

Extracted Range Data

```
(1-1)
Eigenvalues of covariance matrix
 0.719110  32.453365  39.689041
This surface is a curved surface
Coefficients of the quadratic term
 x2 0.002091  y2 0.002354  z2 0.004148
Constant term 6.00132
```

Output Result

Fig. 5.3 A yellow sphere

```
(1-1)
Eigenvalues of covariance matrix
 0.582200  46.676987  68.261543
This surface is a curved surface
Coefficients of the quadratic term
 x2 -0.058997  y2 -0.005652  z2 0.314960
Constant term  0.370584
```

Output Result

Fig. 5.4 A large blue cone

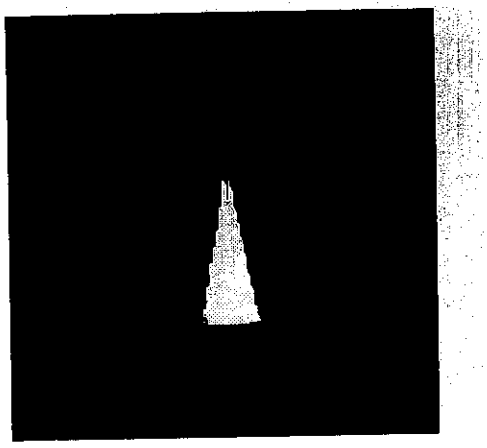

Segmented Colour Image

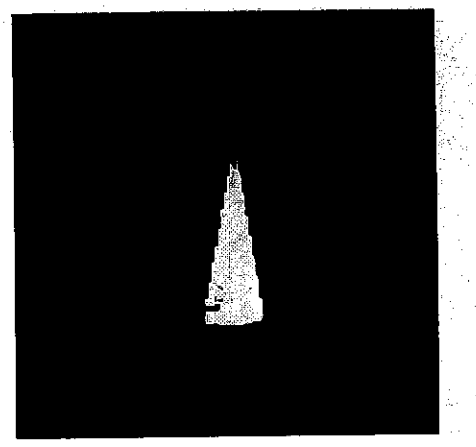

Segmented Colour Image

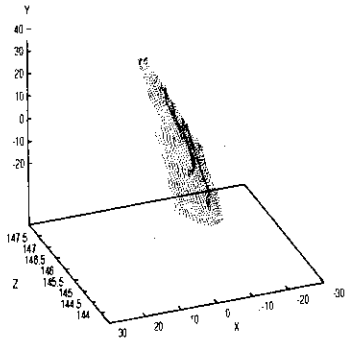

Extracted Range Data

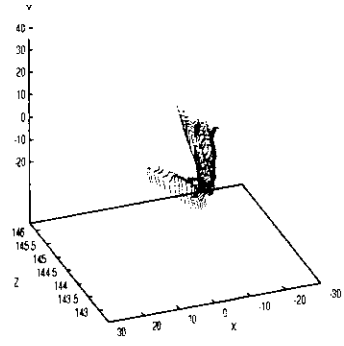

Extracted Range Data

```
(1-1)
Eigenvalues of covariance matrix
 0.166113   16.673960   68.373955
This surface is a curved surface
Coefficients of the quadratic term
 x2 -3.776285   y2 -0.249646   z2 34.224819
Constant term   -0.0154743
```

Output Result

Fig. 5.5 A small red cone

```
(1-1)
Eigenvalues of covariance matrix
 0.226936   18.513708   85.492081
This surface is a curved surface
Coefficients of the quadratic term
 x2 -0.002047   y2 -0.078649   z2 0.496723
Constant term -0.709607
```

Output Result

Fig. 5.6 A declined small red cone

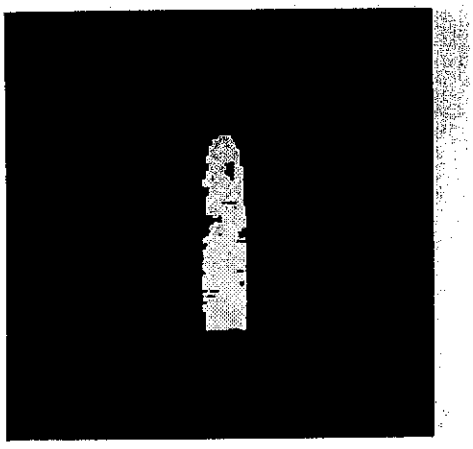

Segmented Colour Image

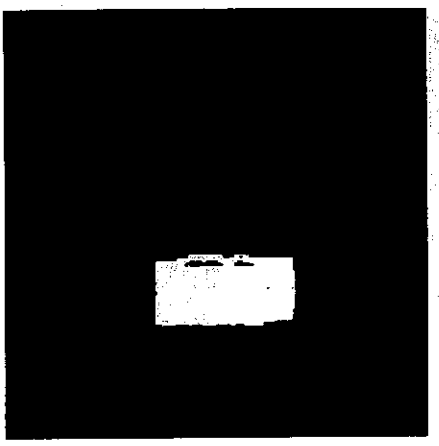

Segmented Colour Image

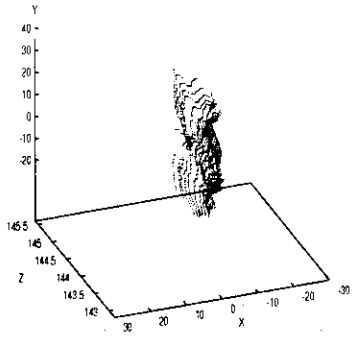

Extracted Range Data

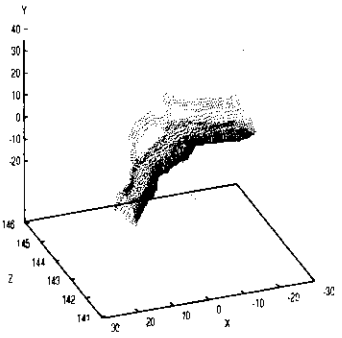

Extracted Range Data

```
(1-1)
Eigenvalues of covariance matrix
 0.183640   15.816867   147.380829
This surface is a curved surface
Coefficients of the quadratic term
 x2 0.000285   y2 0.015828   z2 0.115138
Constant term   2.88602
```

Output Result

Fig. 5.7 A standing green cylinder (a)

```
(1-1)
Eigenvalues of covariance matrix
 0.421317   18.270599   181.796448
This surface is a curved surface
Coefficients of the quadratic term
 x2 -0.000371   y2 0.006646   z2 0.011031
Constant term   14.0234
```

Output Result

Fig. 5.8 A laying green cylinder (2)

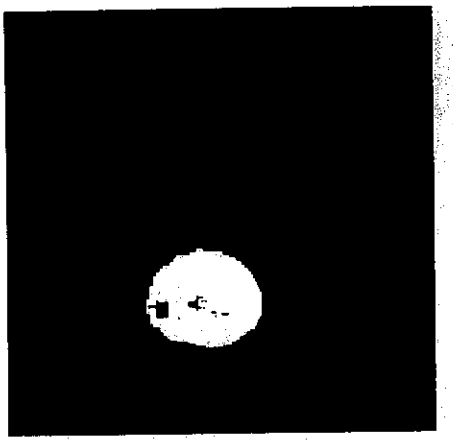

Segmented Colour Image

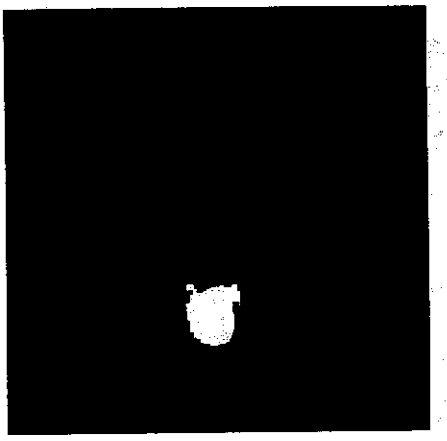

Segmented Colour Image

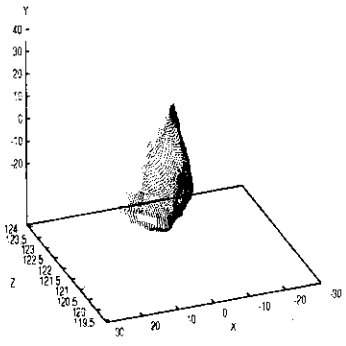

Extracted Range Data

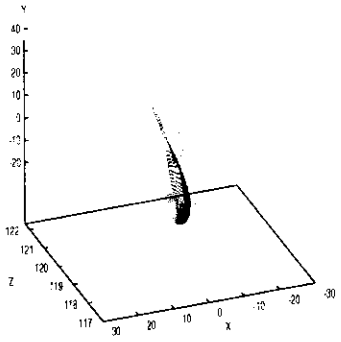

Extracted Range Data

```
(1-1)
Eigenvalues of covariance matrix
 0.294472  20.814297  65.234955
This surface is a curved surface
Coefficients of the quadratic term
 x2 0.005850  y2 0.002760  z2 0.044435
Constant term  3.12328
```

Output Result

Fig. 5.9 A red ellipsoid (b)

```
(1-1)
Eigenvalues of covariance matrix
 0.199150  8.933724  15.981799
This surface is a curved surface
Coefficients of the quadratic term
 x2 -0.002897  y2 -0.002569  z2 0.002131
Constant term  -15.2349
```

Output Result

Fig. 5.10 A red ellipsoid (2)

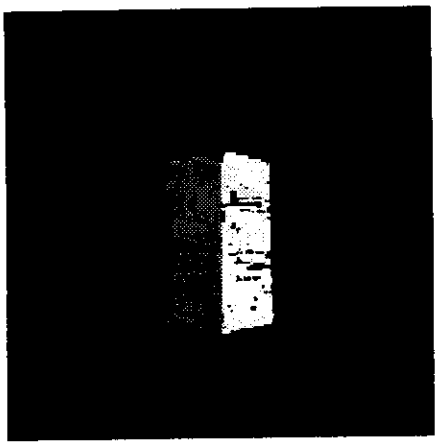

Segmented Colour Image

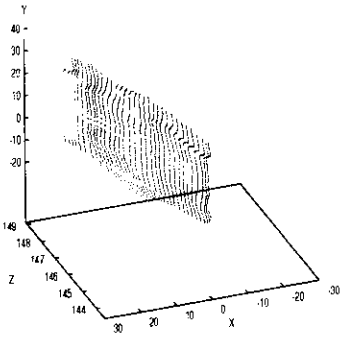

Extracted Range Data (1-1)

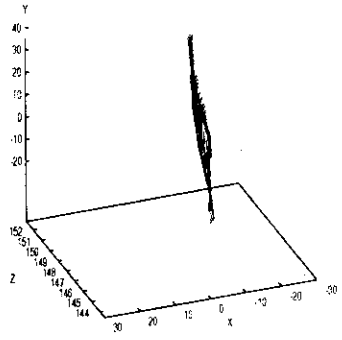

Extracted Range Data (1-2)

```
(1-1)
Eigenvalues of covariance matrix
 0.048275  28.988218  139.505661
This surface is a curved surface
Coefficients of the quadratic term
 x 0.304114  y -0.007185  z -0.952608
```

Output Result (1-1)

```
(1-2)
Eigenvalues of covariance matrix
 0.052308  33.046368  135.363708
This surface is a curved surface
Coefficients of the quadratic term
 x -0.495933  y -0.016018  z -0.868213
```

Output Result (1-2)

Fig. 5.11 A green rectangular solid

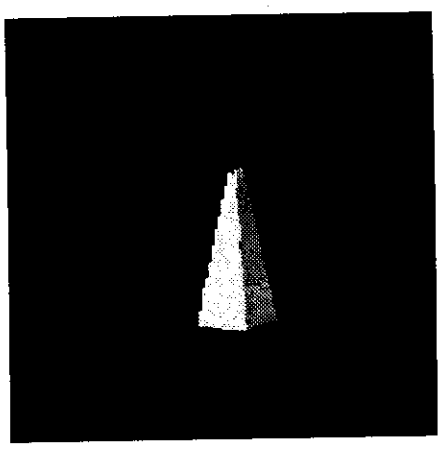

Segmented Colour Image

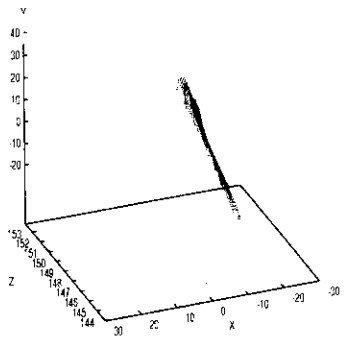

Extracted Range Data (1-1)

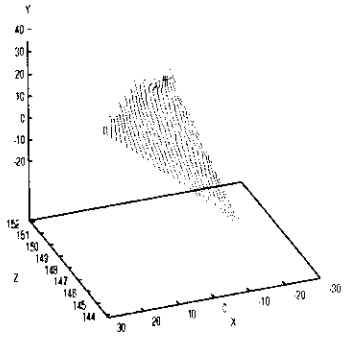

Extracted Range Data (1-2)

```
(1-1)
Eigenvalues of covariance matrix
 0.071715  10.580561  105.578568
This surface is a plane
Normal vector of the plane
 x -0.618977  y -0.157140  z -0.769528
```

Output Result (1-1)

```
(1-2)
Eigenvalues of covariance matrix
 0.071715  10.580561  105.578568
This surface is a plane
Normal vector of the plane
 x 0.457624  y -0.102134  z -0.883261
```

Output Result (1-2)

Fig. 5.12 A yellow pyramid with three side surfaces

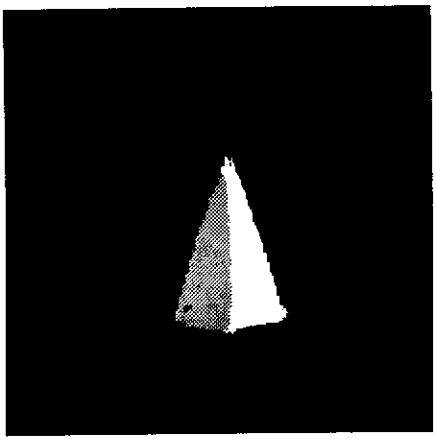

Segmented Colour Image

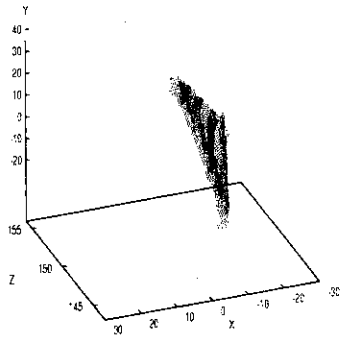

Extracted Range Data (1-1)

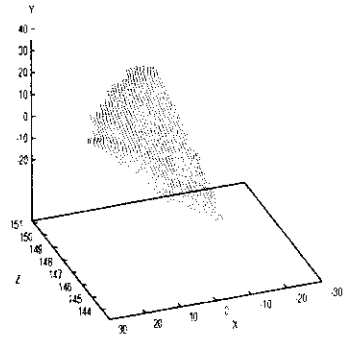

Extracted Range Data (1-2)

```
(1-1)
Eigenvalues of covariance matrix
 0.051695  23.961996  115.042694
This surface is a plane
Normal vector of the plane
 x -0.481948  y -0.186473  z -0.856128
```

Output Result (1-1)

```
(1-2)
Eigenvalues of covariance matrix
 0.044269  21.133184  84.222084
This surface is a plane
Normal vector of the plane
 x 0.341124  y -0.170446  z -0.924437
```

Output Result (1-2)

Fig. 5.13 A yellow pyramid with four side surfaces

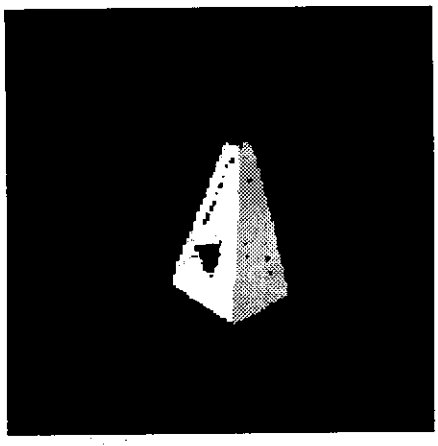

Segmented Colour Image

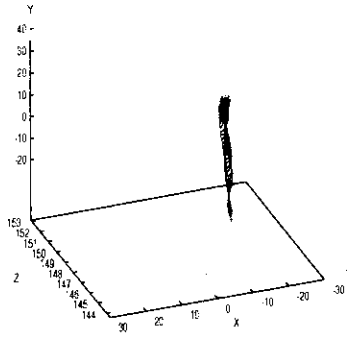

Extracted Range Data (1-1)

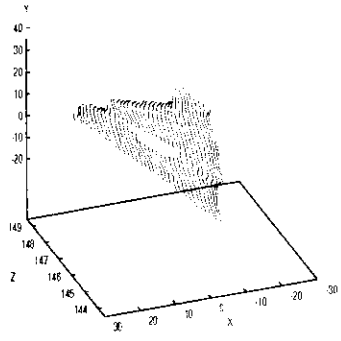

Extracted Range Data (1-2)

```
(1-1)
Eigenvalues of covariance matrix
 0.031987  24.208107  110.935730
This surface is a plane
Normal vector of the plane
 x -0.441871  y 0.002404  z -0.897075
```

Output Result (1-1)

```
(1-2)
Eigenvalues of covariance matrix
 0.027092  27.585974  109.193413
This surface is a plane
Normal vector of the plane
 x 0.280066  y -0.050900  z -0.958630
```

Output Result (1-2)

Fig. 5.14 A declined yellow pyramid with four side surfaces

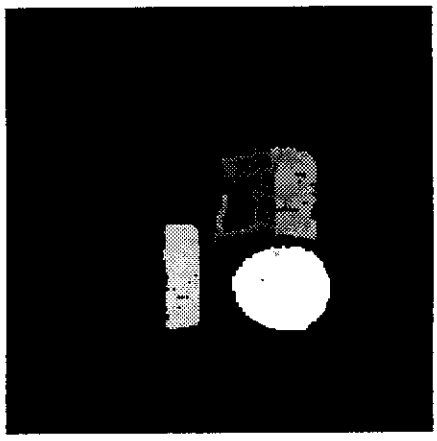

Segmented Colour Image

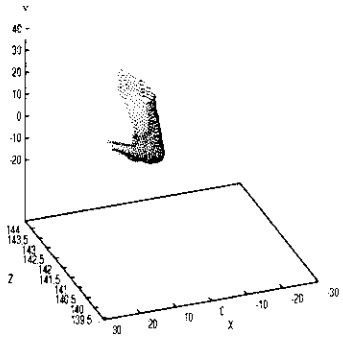

Extracted Range Data (1-1)

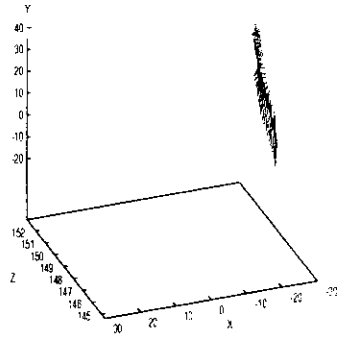

Extracted Range Data (1-2)

```
(1-1)
Eigenvalues of covariance matrix
 0.362105  23.219616  25.529148
This surface is a curved surface
Coefficients of the quadratic term
 x2 0.000154  y2 0.000172  z2 0.000010
Constant term 138.332
```

Output Result (1-1)

```
(2-2)
Eigenvalues of covariance matrix
 0.055463  28.050434  41.513943
This surface is a plane
Normal vector of the plane
 x -0.465489  y -0.005299  z -0.885038
```

Output Result (2-2)

Fig. 5.15 A combination of a red ellipsoid, a blue rectangular solid, a green cylinder, a yellow sphere and a red cone (a)

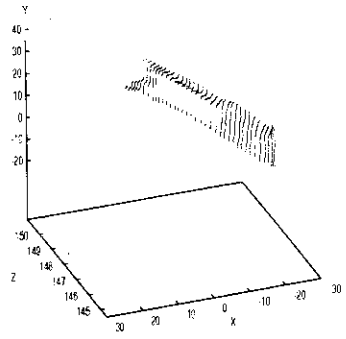

Extracted Range Data (2-3)

```
(2-3)
Eigenvalues of covariance matrix
 0.028790  35.970409  42.885822
This surface is a plane
Normal vector of the plane
 x 0.309622  y 0.016020  z -0.950725
Constant term  -0.697695
```

Output Result (2-3)

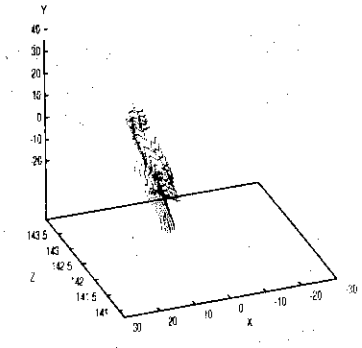

Extracted Range Data (3-4)

```
(3-4)
Eigenvalues of covariance matrix
 0.168471  11.186955  42.902649
This surface is a curved surface
Coefficients of the quadratic term
 x2 0.002325  y2 0.035532  z2 0.440615
Constant term 1.43167
```

Output Result (3-4)

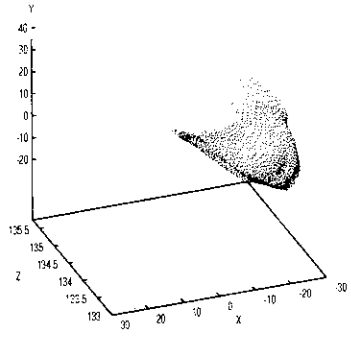

Extracted Range Data (4-5)

```
(4-5)
Eigenvalues of covariance matrix
 0.418079  20.004082  62.773010
This surface is a curved surface
Coefficients of the quadratic term
 x2 0.001639  y2 0.004285  z2 0.013236
Constant term 4.74158
```

Output Result (4-5)

Fig. 5.16 A combination of a red ellipsoid, a blue rectangular solid, a green cylinder, a yellow sphere and a red cone (b)

# 6. Conclusions and Discussions

This report described the study of identification of geometrically shaped solids using colour information and range information. The colour image could be segmented comparatively easily and effectively into each region with the surface of solids using both colour and range information. Segmentation of the colour image was carried out in two steps. One is segmentation using colour information and the other is that using the normal vector which is calculated using 3D range data. Therefore it was avoided to fit the curved surface equation to the extracted range data of plane surfaces of solids with the roof edge.

Range data of each solid could be extracted by using the segmented colour image as a filter. As for identifying geometrically shaped solids, it became possible to distinguish between the plane surface and the curved surface using the minimum eigenvalue of covariance matrix of the distribution of the extracted 3D range data for the surface of each solid. It became possible to identify the side curved surface of the cone using the absolute value of the constant term of the standard form of the quadratic curved surface equation.

The surface of each solids except the cone has not been identified. Since the coefficients of the quadratic equation may be useful in order to identify the surface of other solids with the curved surface, that needs to be discussed furthermore. As for the solids which are formed by plane surfaces, it also need to discuss the suitable method for identifying them.

In this study, it is assumed that the solid has the geometrical convex shape and unique colour. However these restrictions is not suitable for considering recognition of equipment in nuclear plants. Therefore it is necessary to ease these restrictions to make the developed program identify more general solids.

# 7. Future works

This section describes ideas which are considered as future works and is attached to supplement the original Technical Report for Monash University.

The developed program in this report uses the range data and the colour data which are taken by the laser rangefinder and the colour CCD camera of Monash University respectively. This range data includes much noise because the rangefinder was developed for obstacle avoidance in mobile robot navigation. Thus accuracy of the range data is not so high and much effort is necessary for noise reduction to utilize this range data for object recognition. However the range data which is taken by the sensing system[13] developed in JAERI include less noise than the range data taken by the rangefinder of Monash University though it takes longer time to detect range data. The sensing system can also take the colour image. The colour CCD camera of sensing system is also used for rangefinding so that the range image can be overlaid on the colour image automatically while in this program this process is done manually as describing in section 4.2. Therefore I am considering to process the range data and the colour image which are taken by the sensing system using the developed program in this report if I had chance.

Another idea is for sensor fusion of colour data and range data. The developed program uses the colour data and range data complementarily for segmentation of the colour image. Thus colour data and range data are integrated in the sense of the paper[1]. However they have not been fused essentially because they are used separately. I think that colour data and range data would be fused essentially if both data were processed in same way in a program. I am considering the application of the method for segmentation using range data to segmentation using colour data as one realization of essential fusion of colour and range data. In other words, colour data is used as data of the geodesic dome histogram in place of range data. In the case of using range data, two components is needed for specifying the orientation of one normal vector of the surface. These two components may be replaced by hue and saturation respectively. Although it can be considered to use intensity in place of saturation, I think that saturation is better than intensity because of including a part of colour attribution. If segmentation of the colour image using colour geodesic dome could work, the two information, that is colour and range informations, become processed in the same way. Furthermore, if hypersphere geodesic dome which is embedded in the five-dimensional space could be realized in the computer, two information would be processed on same geodesic dome simultaneously. I think that this may be one of true fusion of colour and range information.

## Acknowledgements

I thank Professor R. Jarvis, Dr. M.Takatsuka, other staffs and students in the department of Electrical and Computer Systems Engineering of Monash University. I thank for much support of staffs of JRDC and people of JAERI.

### Reference

[1] *Journal of the Robotics Society of Japan*, **Vol.8**, no.6 (1990).

[2] K.Ajay, "*Active Rangefinding for Mobile Robot Navigation*", Ph.D thesis (Dept.of E&CSE in Monash University, 1993).

[3] R.C.Gonzalez, R.E.Woods, "*Digital Image Processing*", (ADDISION-WESLEY PUBLISHING COMPANY, 1993).

[4] H.R.Myler, A.R.Weeks, "*THE POCKET HAND BOOK OF IMAGE PROCESSING ALGORITHMS IN C*", (Prentice Hall P T R, 1993).

[5] R.Jarvis, private communication.

[6] W. Mendenhall, D.D. Wackerly, R.L. Scheaffer, "*Mathematical Statistics with Applications*" (Duxbury Press, 1990).

[7] "*HAND BOOK OF IMAGE ANALYSIS*" (University of Tokyo Press,1994).

[8] T.Uchiyama, M.A.Arbib,"*Color Image Segmentation Using Competitive Learning*", IEEE Trans.on Pattern Analysis and Machine Intelligence,**Vol.16**,No.12, pp.1197-1206(1994).

[9] B. K. P. Horn, "*Robot Vision*" (The MIT Press,1986).

[10] M.J.Wenninger, "*Spherical Models*" (Cambridge University Press,1979).

[11] N. Yokoya and M. D. Levine, "*Range Image Segmentation Based on Differential Geometry: A Hybrid Approach*", McRCIM-TR-CIM 87-16 (1987).

[12] P. J. Besl and R. C. Jain, "*Invariant Surface Characteristics for 3D Object Recognition in Range Images*", Computer vision, graphics and Image processing **33**, pp. 33-80 (1986).

[13] K. Ebihara, "*The Conceptual Design of the Sensing System for Patrolling and Inspecting a Nuclear Facility by the Intelligent Robot*", (JAERI-M 93-225, 1993)

## Acknowledgements

I thank Professor R. Jarvis, Dr. M.Takatsuka, other staffs and students in the department of Electrical and Computer Systems Engineering of Monash University. I thank for much support of staffs of JRDC and people of JAERI.

### Reference

[1] *Journal of the Robotics Society of Japan*, **Vol.8**, no.6 (1990).

[2] K.Ajay, "*Active Rangefinding for Mobile Robot Navigation*", Ph.D thesis (Dept.of E&CSE in Monash University, 1993).

[3] R.C.Gonzalez, R.E.Woods, "*Digital Image Processing*", (ADDISION-WESLEY PUBLISHING COMPANY, 1993).

[4] H.R.Myler, A.R.Weeks, "*THE POCKET HAND BOOK OF IMAGE PROCESSING ALGORITHMS IN C*", (Prentice Hall P T R, 1993).

[5] R.Jarvis, private communication.

[6] W. Mendenhall, D.D. Wackerly, R.L. Scheaffer, "*Mathematical Statistics with Applications*" (Duxbury Press, 1990).

[7] "*HAND BOOK OF IMAGE ANALYSIS*" (University of Tokyo Press,1994).

[8] T.Uchiyama, M.A.Arbib,"*Color Image Segmentation Using Competitive Learning*", IEEE Trans.on Pattern Analysis and Machine Intelligence,**Vol.16**,No.12, pp.1197-1206(1994).

[9] B. K. P. Horn, "*Robot Vision*" (The MIT Press,1986).

[10] M.J.Wenninger, "*Spherical Models*" (Cambridge University Press,1979).

[11] N. Yokoya and M. D. Levine, "*Range Image Segmentation Based on Differential Geometry: A Hybrid Approach*", McRCIM-TR-CIM 87-16 (1987).

[12] P. J. Besl and R. C. Jain, "*Invariant Surface Characteristics for 3D Object Recognition in Range Images*", Computer vision, graphics and Image processing **33**, pp. 33-80 (1986).

[13] K. Ebihara, "*The Conceptual Design of the Sensing System for Patrolling and Inspecting a Nuclear Facility by the Intelligent Robot*", (JAERI-M 93-225, 1993)

# Appendix 1 Range Image Segmentation using Curvatures

Segmentation of the range image using curvatures is described in this appendix. The program for segmentation of the image was developed on the basis of the paper [11]. Although this program was not used for segmenting the colour image in this project, the possibility of using surface curvature information could be checked.

In this program, two curvatures such as Gaussian curvature $K$ and mean curvature $H$ are used for segmenting the range image. Since these curvatures can be obtained by fitting the quadratic curved surface to a certain local region of the curved surface. In other words, the local region of the curved surface is regarded as the patch of the quadratic curved surface approximately. According to the paper[12], the quadratic curved surface can be classified into eight types of surfaces based on the sign of mean curvature and Gaussian curvature. In Figure A.1, each type of the quadratic curved surface and the corresponding combination of signs of mean curvature and Gaussian curvature are shown. Using these types of the quadratic curved surface, patches on the surface of the range image are classified into eight kinds of region.

In the developed program, coefficients of the general form of the quadratic curved surface equation in Equation A.1 are calculated by fitting window operators to the local region, that is patch, of the range image.

$$z(x, y) = ax^2 + by^2 + cx + dy + e. \tag{A.1}$$

Two curvatures, that is mean curvature and Gaussian curvature, are calculated using obtained coefficients a, b, c and d. The window operator whose sizes are $3 \times 3$, $5 \times 5$ and $7 \times 7$ respectively was used of calculating coefficients by scanning on the range image. To checking usefulness of curvature information for segmenting the range image(Figure A.2), the synthetic range image was used as the sample range image. In the case of using the synthetic range image, the noise influence on segmentation can be estimated quantitatively. In Figure A.3, A.4 and A.5, the results of segmenting the synthetic range image of a hemisphere including Gaussian noise with the standard deviation $\sigma$ are shown. According to this figure, the robustness of segmentation for Gaussian noise increases as the size of the window operator is large. However the range image including more than 0.01% noise of range data cannot be segmented well even by using $7 \times 7$ window operator. Hence it is found that the calculation of curvature is sensitive to included noise. As investigating noise included in the real range data in Section 3, the standard deviation of range data of the plane at 100cm distance after smoothing by 1 time iteration of the arithmetic mean filer with $9 \times 9$ size is 0.52 $cm^2$. Then about 0.7% noise is included in the smoothed range data. Hence the segmentation using curvature information is not useful for real range data which is detected by the laser-scanning rangefinder.

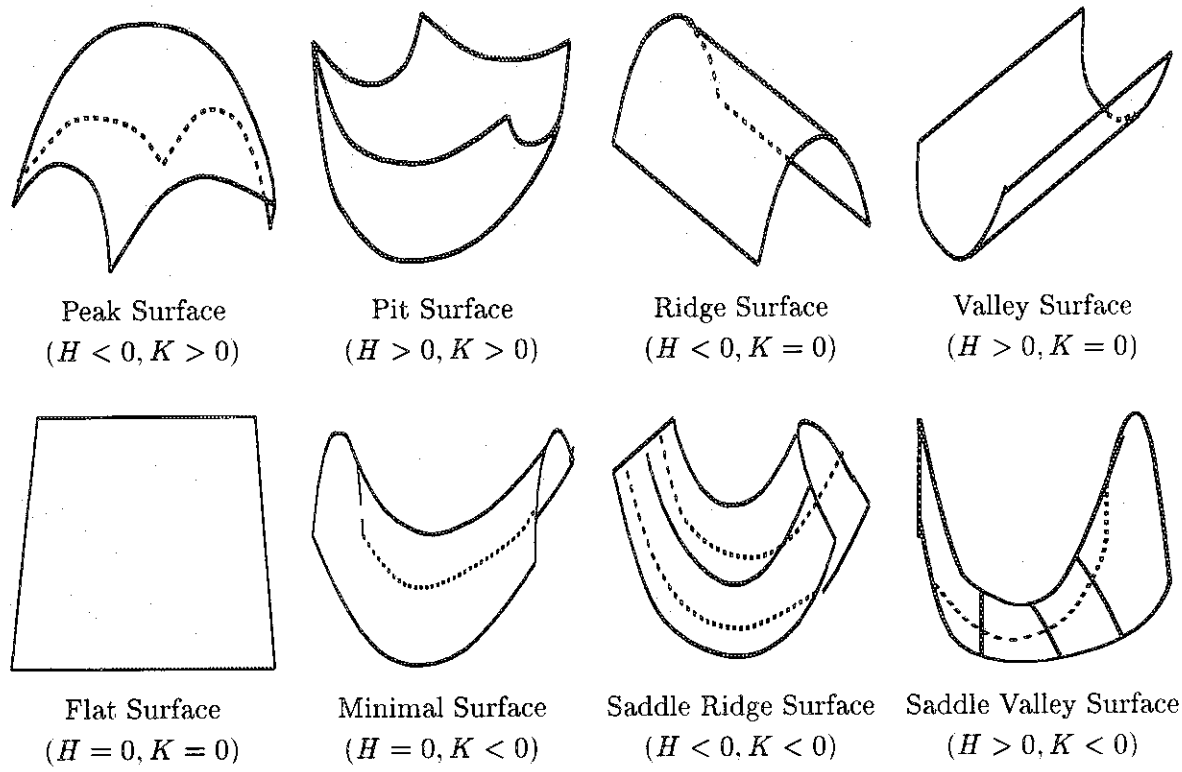


Fig. A.1 Eight Surface Types

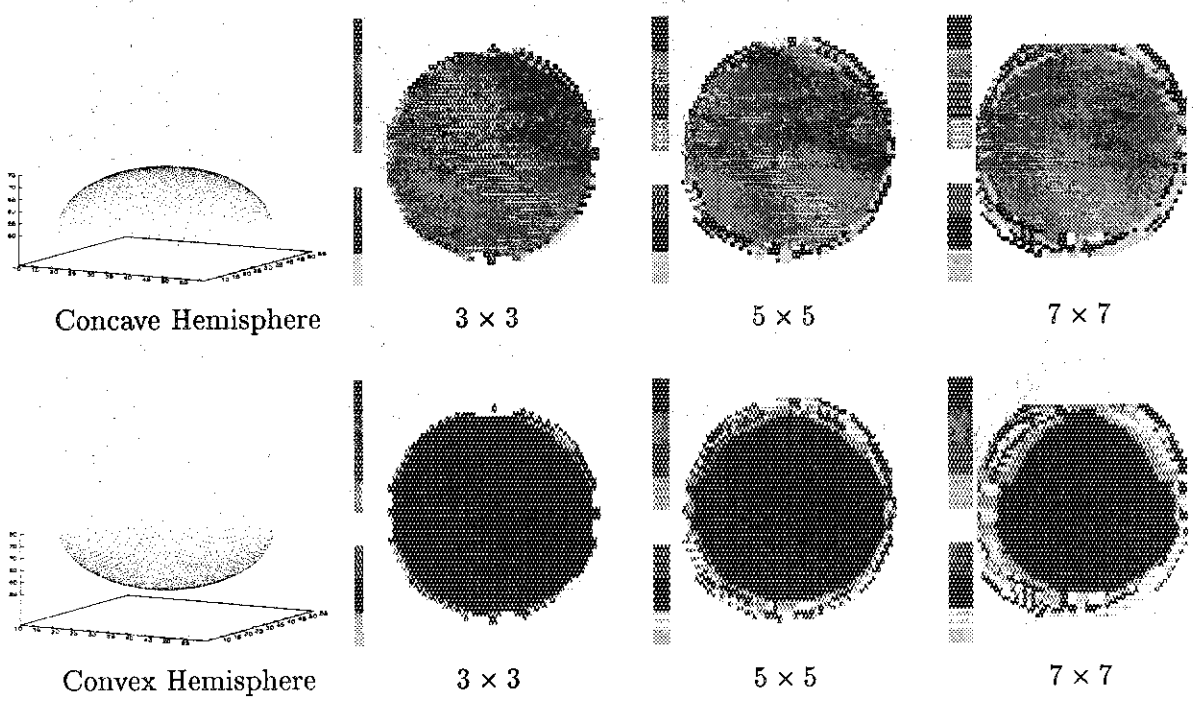


Fig. A.2 Calculation result : The surface type is assigned using Gaussian curvature and mean curvature calculated by the algorithm of Yokoya et al[2]. The peak, pit, ridge. valley, flat, minimal, saddle ridge and saddle valley surface are represented respectively by the gray level from the top to the bottom in the side bar.

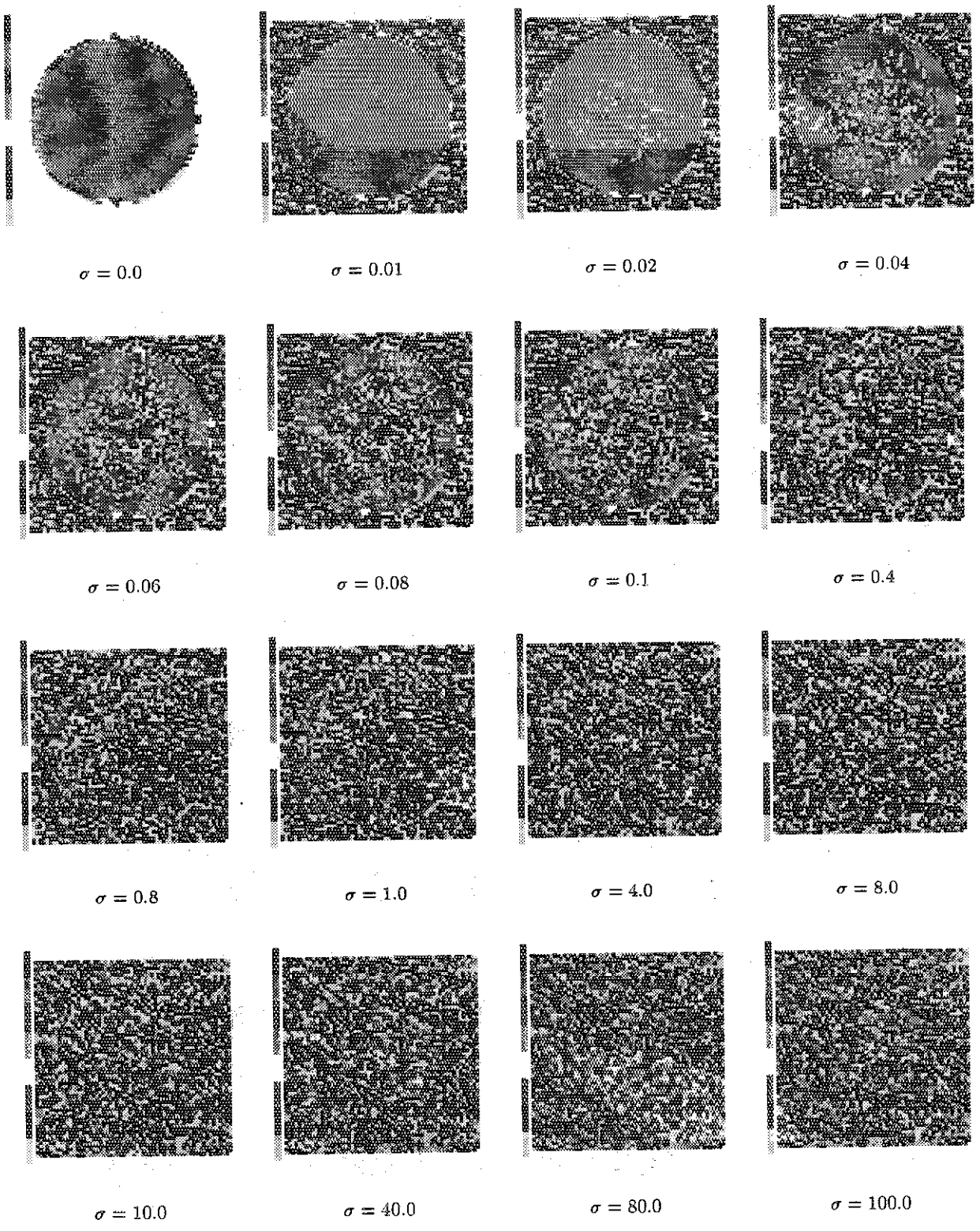


Fig. A.3 Visual representation of the influence of added noise to the synthetic range image of the concave hemisphere(The window size is 3 × 3) The curvatures are calculated using the synthetic range image to which Gaussian noise with the standard deviation $\sigma$ is added.

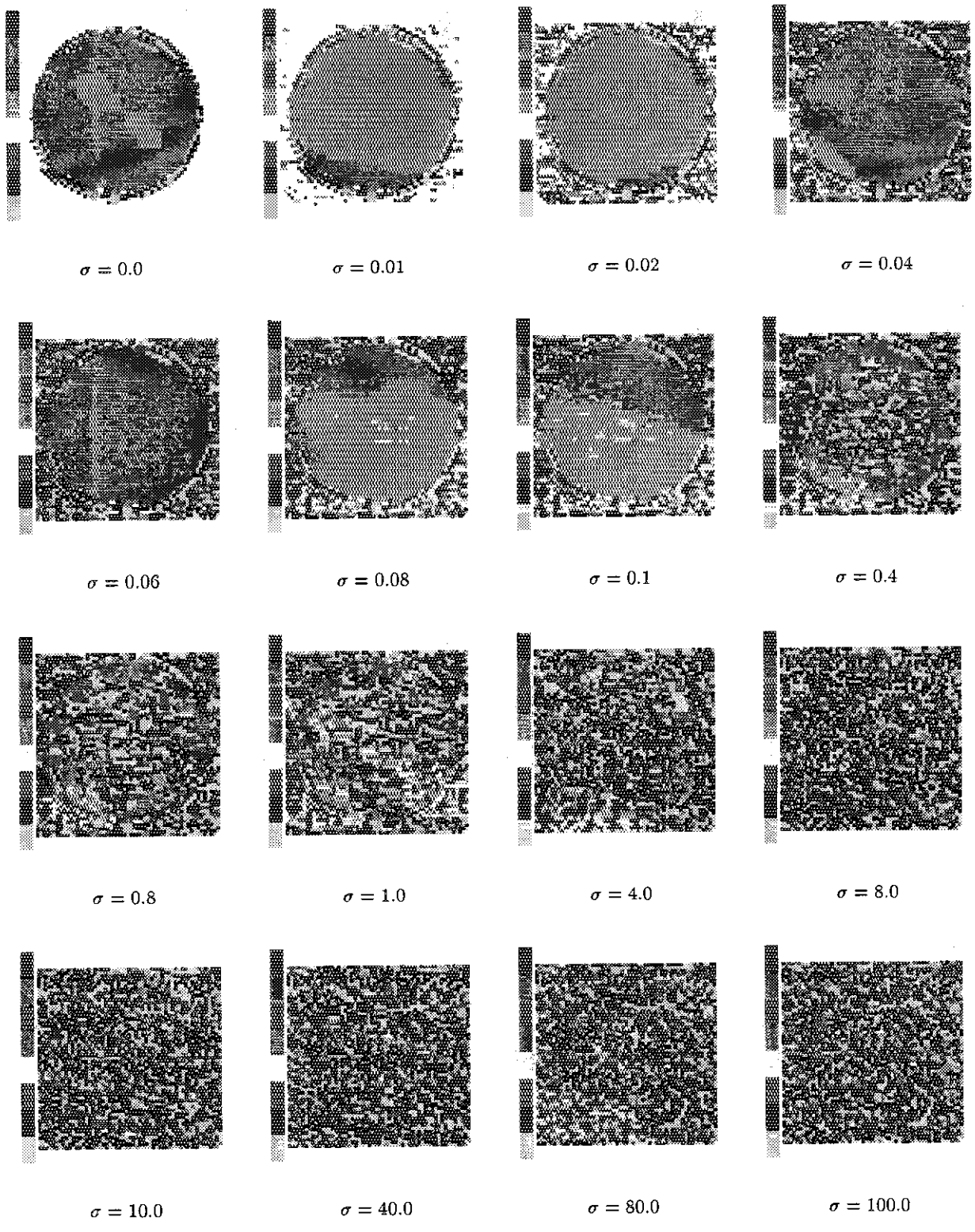


Fig. A.4 Visual representation of the influence of added noise to the synthetic range image of the concave hemisphere (The window size is 5 × 5)

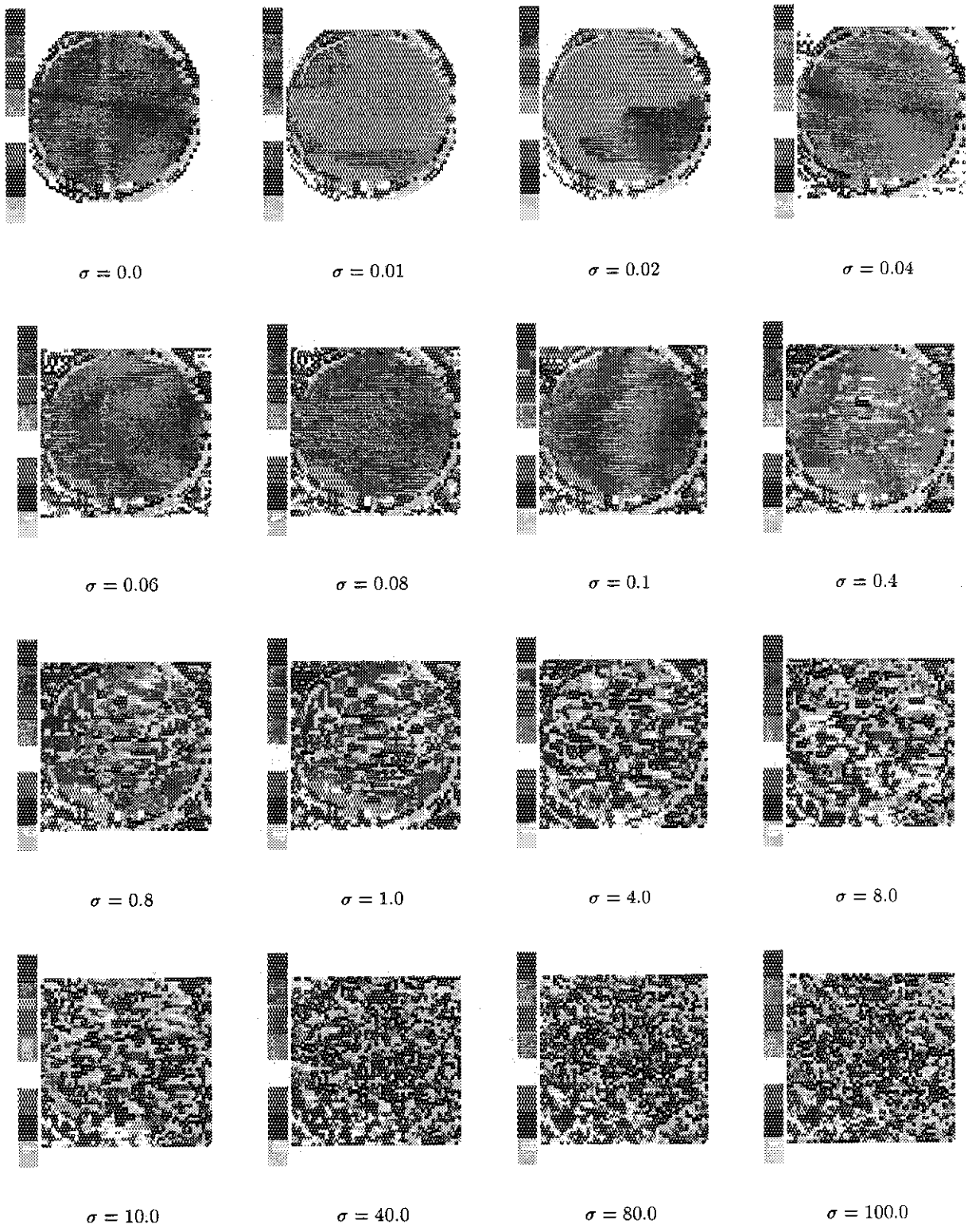


Fig. A.5 Visual representation of the influence of added noise to the synthetic range image of the concave hemisphere (The window size is 7 × 7)